NASA Contractor Report 178146

NASA-CR-178146
19860020997

NOISE PREDICTIONS OF A HIGH BYPASS TURBOFAN ENGINE USING THE LOCKHEED NEAR-FIELD NOISE PREDICTION PROGRAM

John W. Rawls, Jr.

PRC Kentron, Inc.
Aerospace Technologies Division
3221 North Armistead Avenue
Hampton, VA 23666

CONTRACT NAS1-18000
July 1986

National Aeronautics and
Space Administration

Langley Research Center
Hampton, Virginia 23665

Table of Contents

SUMMARY

This report examines the prediction of engine noise during cruise using the Near-Field Noise Prediction Program developed by Lockheed. Test conditions were established which simulate the operation of a high bypass turbofan engine under a wide range of operating conditions. These test conditions include variations in altitude, flight Mach number and thrust setting. Based on the results of noise prediction made using the Lockheed program, an evaluation of the impact of these test conditions on the OASPL and the one-third octave band spectra is made. An evaluation of the sensitivity of flight condition parameters is also made.

The primary noise source from a high bypass turbofan was determined to be fan broadband shock noise. This noise source can be expected to be present during normal cruising conditions. When present, fan broadband shock noise usually dominates at all frequencies and all directivity angles. Other noise sources of importance are broadband shock noise from the primary jet, fan noise, fan mixing noise and turbine noise.

INTRODUCTION

The prediction of the near-field noise environment of an aircraft in cruise has become an important element in the research and development of wing designs that can maintain laminar flow at a cruise speed of Mach .8. An acoustic disturbance with the correct frequency and intensity is known to cause transition of a laminar boundary layer under laboratory conditions (ref. 1). It is not known whether engine noise, airframe noise, or some unidentified noise source from the aircraft will have the correct characteristics to cause boundary layer transition under flight conditions. For the next generation of passenger aircraft to successfully employ laminar flow wing designs, it must first be determined if noise from the current high bypass turbofans or the proposed propfans will cause boundary layer transition.

To investigate these questions, the dominant noise sources in the near-field of the aircraft must be identified. The purpose of this report is to obtain an estimate of these noise sources. Using the near-field noise prediction program developed by Lockheed (ref. 2, 3, 4), the propulsion noise sources of a typical high bypass turbofan are predicted and evaluated. Based on these results, recommendations for improving the predictions are made.

LIST OF SYMBOLS

Symbols

A	Jet stretching parameter
c	Speed of sound, ft/sec
f	Frequency, Hz
k	Wave number; $k = 2\pi f/c$
L_f	Jet potential core length (in flight), ft
L_s	Jet potential core length (stationary), ft
ℓ	Exponent of shock cell strength parameter β
M	Mach number
M_a	Aircraft Mach number
$\dot{m}$	Mass flow rate, lbm/sec
R	Universal gas constant 1716.55, $ft^2/sec^2\ °R$
r	Source to observer distance, ft
T	Temperature, °R
V	Velocity, ft/sec
α	Potential core stretching factor; $\alpha = L_f/L_s$
β	Shock cell strength parameter
γ	Ratio of specific heats; $\gamma = 1.4$
ρ	Density, lbm/ft^3
ϕ	Observer angle, degrees
ϕ'	Emission angle, degrees

Subscripts

a	Ambient
e	Equivalent
f	Flight
j	Jet
p	Primary
ref	Reference
s	Secondary

LOCKHEED NEARFIELD NOISE PREDICTION PROGRAM

The Lockheed Near-Field Noise Prediction Program (ref. 2, 3, 4), released in the fall of 1979, was developed as a means of predicting the near-field noise environment of an aircraft in cruise. Noise sources are divided into two groups, propulsion sources and airframe sources. The propulsion noise sources include the fan, compressor, core, turbine and jet. The airframe sources consist of trailing edge noise and turbulent boundary noise.

The algorithms used to predict the noise sources are, with the exception of the jet mixing noise, far-field static prediction methods with modification for forward flight effects. The acoustic far-field is defined as a function of the source type (monopole, dipole, or quadrapole), source frequency, and ambient sound speed. Swift and Mungur indicate (ref. 4) that for practical purposes, the division between the acoustic near-field and far-field occurs when

$$\begin{aligned} kr &= 1 \quad \text{for monopoles} \\ kr &= 2 \quad \text{for dipoles} \\ kr &= 3 \quad \text{for quadrapoles} \end{aligned} \tag{1}$$

where the wave number $k = 2\pi f/c$ and r is the source-to-observer distance. Figure 1 shows the division of the near-field and far-field at 30,000 feet, where the speed of sound is 994.85 feet/sec. At 30,000 feet, this approximation is not a major restriction for monopoles and dipoles. The major quadrapole source is jet mixing noise for which there is a near-field prediction method. At sea level, the division between far-field and near-field requires greater distance r, since the ambient speed of sound is greater.

One-third octave band spectra from 50 to 12,500 Hz are predicted for each noise source as well as the Overall Sound Pressure Level (OASPL) of each observer location. The observer directivity angle may vary from 0° to 180° for all noise sources except jet mixing noise. Observer locations are not allowed in the mixing region of the jet and the ambient air.

Input to the Lockheed program is divided into two parts. The first is configuration input which describes the physical parameters of the engine, i.e., engine length, number of fan blades, etc. The second is flight condition input which describes the atmospheric conditions, the specific operating condition of the engine and the flight speed for each flight condition of interest.

MODIFICATION FOR FORWARD FLIGHT

The following modifications transform static predictions to flight predictions.

Coordinate Transformation

The first modification is a coordinate transformation which defines the relationship between the observer angle and source-to-observer distance at the time the sound is received and the emission angle and propagation distance at the time the sound is emitted. The relationship between observer angle ϕ and emission angle ϕ' and observer distances r and r' are given by the following equation

$$\phi' = \cot^{-1}\left\{\frac{1}{1 - M_a^2}\left[\cot \phi + M_A \sqrt{1 - M_a^2 + \cot^2 \phi}\right]\right\} \tag{2}$$

and

$$r' = r \frac{\sin \phi}{\sin \phi'} \tag{3}$$

Figure 2 shows the geometric relationship of these coordinates.

Convective Amplification

Convective amplification accounts for the change in the acoustic intensity of a moving source from that of a stationary source. In the Lockheed program, the modification for convective amplification is given by

$$CA = 40 \text{ Log } \left(\frac{1}{1 - M_a \cos \phi'}\right) \tag{4}$$

Experimental verification of this effect has been observed for engine components including the fan, core, turbine and broadband shock noise (ref. 5, 6, 7). As shown in figure 3, however, with a cruising Mach number of 0.8 and an emission angle of 30°, the sound pressure level (SPL) is increased by 20.5 dB. As a result of the rather large increase in the sound pressure level, experimental validation at these speeds is required.

Dynamic Amplification

Dynamic application is an effect which applies only to distributed sources such as jet mixing noise and turbulent boundary layer noise. This effect, which occurs in addition to convective amplification, is given by

$$DA = 10 \text{ Log } \left(\frac{1}{1 - M_a \cos \phi'}\right) \tag{5}$$

Like convective amplification, dynamic amplification causes an increase in the sound pressure level for emission angles less than 90°. As shown in figure 4, a flight Mach number of 0.8 and an emission angle of 30° will result in an increase in the sound pressure level of 5 dB.

The jet mixing noise algorithm has convective amplification built into the model, and the authors of the Lockheed program included dynamic amplification as an addition flight effect to this model.

Dynamic amplification has been removed from the broadband shock noise model for this study since, according to Swift and Mugar, it does not apply to broadband shock noise.

Doppler Frequency Shift

The last modification is a doppler frequency shift to account for the change in the source true frequency and the observed frequency of a moving source and observer. The expression which relates the source true frequency to the observer detected frequency in a stationary medium where both observer and source are in parallel motion is

$$f_o = f_s \frac{c_a + |V_m| \cos \theta}{c_a + |V_s| \cos \theta} \tag{6}$$

where

f_o = observer detected frequency

f_s = source true frequency

c_a = ambient speed of sound

V_m = moving observer velocity

V_s = moving source velocity

θ = angle between source and observer

For point sources such as a fan, core, turbine, or jet broadband shock noise, the noise source and an observer on the aircraft are moving at the same speed and in the same direction. Therefore, no frequency adjustment is required. A frequency shift is required for distributed source such as jet mixing noise and turbulent boundary layer noise since the distributed sources move at a different speed from the aircraft. However, this effect is not included in Lockheed program for these two sources.

HIGH BYPASS TURBOFAN MODEL DESCRIPTION

To obtain reasonable estimates of the required input parameters, a model high bypass turbofan has been formulated using estimated performance parameters from a full scale high bypass turbofan with a maximum continuous thrust rating of 38000 lb. The configuration parameters of the engine are listed in Table 1.

Temperature and pressure ratios were obtained for the fan discharge, the combustor inlet and the low pressure turbine exhaust as a function of flight Mach number, altitude and thrust setting. The corrected rotational speeds of the fan and high pressure compressor, the corrected fan mass flow rate, the bypass ratio, and the fuel mass flow rate are also known. With this information, the necessary input data for a complete noise prediction of a high bypass turbofan were computed.

FLIGHT CONDITION TEST MATRIX

The following 3 sets of flight conditions were established to investigate the noise levels that will be predicted in the near-field using the Lockheed Near-Field Noise Prediction Program.

Altitude Variation

The first set of tests involves varying the altitude from 20,000 to 40,000 feet while operating at maximum continuous thrust and a flight Mach number of 0.8. The changes in atmospheric density, sound speed, pressure, temperature, etc. affect not only the noise predictions, but also the performance calculations of the engine. For example, the mass flow rate through the fan in this set of tests is reduced by 46% at 40,000 feet from the mass flow rate at 20,000 feet due primarily to the decrease in atmospheric density.

Thrust Variation

The second set of tests examines the change in noise levels as the thrust is varied from 100% maximum continuous thrust to 64% of max. thrust in 5 steps while maintaining flight speed of Mach 0.8 and an altitude of 30,000 feet.

Flight Mach Number Variation

In the last set of flight conditions, the flight Mach number is varied from .5 to .9 in increments of .1. Flight speed and altitude are maintained at 0.8 and 30,000 feet, respectively.

Observer Location

These flight conditions will establish the dominant noise sources as predicted by the Lockheed program under a wide range of operating conditions. In each test, predictions are made along a 15 foot side line distance, at four points corresponding to directivity angles of 30°, 60°, 90° and 120°.

Atmospheric conditions are considered to be standard day conditions.

NOISE PREDICTION

Noise predictions were made using the flight condition input listed in Tables 2, 3 and 4. The propulsion noise sources predicted for these tests are forward and aft radiated fan noise, core noise, turbine noise, and jet mixing and broadband shock noise for both the primary and secondary nozzles. Compressor noise was not considered since fan noise is expected to dominate the compressor noise source for both the broadband and the discrete frequency components.

Altitude Variations

Parameters relevant to noise predictions and engine performance vary significantly with altitude as shown in Table 5. Two parameters important to noise predictions that change with altitude are the ambient density ρ_a and speed of sound c_a. The product of these two parameters is the acoustic impedance. Each noise source is corrected for local acoustic impedance variations by a factor

$$IMP = 10 \text{ Log } (\rho_a c_a / \rho_0 c_0) \qquad (7)$$

where $\rho_a c_a$ is the local ambient acoustic impedance and $\rho_0 c_0$ is the standard day sea level reference acoustic impedance. In this study, for example, the decrease in the acoustic impedance from 20,000 to 40,000 feet will result in a 4.4 dB decrease in the OASPL.

Performance parameters are also affected by altitude variations. The most significant change occurs in the fan mass flow rates. At 40,000 feet the fan mass flow rate is 46% lower than it is at 20,000 feet. This reduction in mass flow rate is due to the reduction of the ambient density with increasing altitude. A constant flight speed can be maintained (with reduced mass flow rates at higher altitudes) since drag also decreases with increasing altitude up to about 30,000 feet.

It was expected that the total OASPL would demonstrate a significant change in level with altitude variations. However, this was not the case. As shown in figure 5, the total OASPL is plotted as a function of altitude for observer angles of 30°, 60°, 90° and 120°. The total OASPL is plotted along with the significant sources at each directivity angle. Sources with an OASPL more than 20 dB below the total OASPL do not contribute significantly to the total. In these figures, sources as much as 40 dB below the total are plotted.

In each of these figures, the total OASPL is dominated by the broadband shock noise of the secondary jet, which did not change with altitude. The reason broadband shock noise did not change can be explained as follows. The

broadband shock noise OASPL, whether it is from the fan or the primary jet, is determined primarily by the jet Mach number. In this study, the fan exhaust velocity V_2 and jet total temperature T_2 remained virtually unchanged from 20,000 feet to 40,000, feet while the ambient speed of sound decreased over the same range. This causes an increase in the jet Mach number and, consequently, an increase in the fan broadband shock noise. However, as previously mentioned, each noise source is corrected for variations in the local acoustic impedance. Therefore, the increase in the fan broadband shock noise level due to the jet Mach number is offset by the local acoustic impedance correction.

The broadband shock noise of the primary jet actually increased with altitude. Unlike the jet velocity of the fan, which remained constant, the jet velocity of the primary jet increased with altitude. This, combined with a decreasing sound speed with altitude, results in an increase in the jet Mach number and also an increase in the OASPL.

Forward radiated fan noise does demonstrate the expected decrease in the OASPL with increasing altitude. This is due to the decrease in the fan mass flow previously mentioned.

Thrust Variations

This set of test examines the change in the propulsion noise sources OASPL with thrust setting. As expected, the total OASPL decreases with reduced thrust. As shown in figure 6, the total OASPL is plotted as a function of percent thrust setting for observer angles of 30, 60, 90 and 120°. (Only the most significant are plotted for each observer angle.)

In each of these figures, the dominant noise source is the broadband shock noise of the secondary jet. The remaining propulsion noise source contribute very little to the total OASPL. The reason broadband shock noise of the secondary jet dominates (even at low thrust settings) is due to the relatively low speed of sound in the jet flow. The sound speed in a jet can be expressed as

$$c_j = \sqrt{\gamma R T_j - \left(\frac{\gamma - 1}{2}\right) V_j^2} \tag{8}$$

where T_j is the jet total temperature and V_j is the jet velocity. In order for broadband shock noise to occur, the jet Mach number M_j given by

$$M_j = \frac{V_j}{c_j} \tag{9}$$

must be greater than or equal to one. The jet Mach for the 100% thrust setting is 1.18 and for 64% is 1.11.

Flight Mach Number Variations

An increase in Mach number dramatically increases the noise levels as shown in figure 7. Broadband shock noise increased on the order of 35 dB from Mach .5 to Mach .9 at a directivity angle of 30° as indicated in Table 8. All noise source prediction methods in the Lockheed Near-Field Noise Prediction Program are based on a stationary noise source with modification for forward flight effects.

The most influential of the flight effects modifications is convection amplification. The change in the acoustic intensity of a stationary source to a source in motion in terms of decibels is

$$\Delta dB = 40 \text{ Log } \left(\frac{1}{1 - M_a \cos \phi'}\right) \qquad (10)$$

where M_a is the flight Mach number. This effect will increase the noise level in the forward arc and decrease the level in the aft arc.

Figure 3 shows the variation in noise levels as a function of Mach number due to the convection effect. This accounts for most of the increase in the noise level of the broadband shock noise from $M_a = 0.5$ to $M_a = 0.9$ at 30°. Swift and Mungur point out (ref. 3) that, in light of the large increase in the noise level at high Mach numbers, experimental validations of convective amplification at these speeds is required.

All the noise sources predicted demonstrate significant increase in noise level at all directivity angles with the exception of jet mixing noise. Jet mixing noise of the primary and secondary nozzles decreased with increased flight speed.

Jet mixing noise correlates on the relative Mach number M given by

$$M = M_j\left(1 - \frac{V_a}{V_j}\right)^{3/4} \qquad (11)$$

where M_j is the jet Mach number, V_a is the aircraft velocity and V_j is the jet velocity. Values of the relative Mach number M are given in Table 9 for the five flight Mach numbers. As M_f increases, M decreases resulting in lower jet mixing noise at increased flight speeds.

SOURCE FREQUENCY DISTRIBUTION

All noise sources must be regarded as capable of causing boundary layer transition since the correct frequency and intensity may be obtained from a source which is not dominant. However, in terms of validating this code, it is important to identify the primary noise source during cruise since it is these sources which have the greatest impact on the total noise level.

The propulsion noise sources have been discussed in terms of their OASPL under a variety of flight conditions. Additional insight can be obtained in determining the primary noise sources by examining the one-third octave band spectra. Four test conditions were chosen for comparison. In each test, the spectra of each propulsion noise source is plotted at four directivity angles 30, 60, 90 and 120 degrees. Test 1 establishes the baseline condition for comparison with the remaining three tests. The baseline conditions are flight Mach number 0.8, altitude 30,000 feet and thrust setting of 100%. In tests 2, 3, and 4, one of these parameters is varied as shown in the diagram below to determine the impact on the spectral distribution. For purposes of discussion, the frequency distribution of each noise source will be discussed individually rather than on a test by test basis.

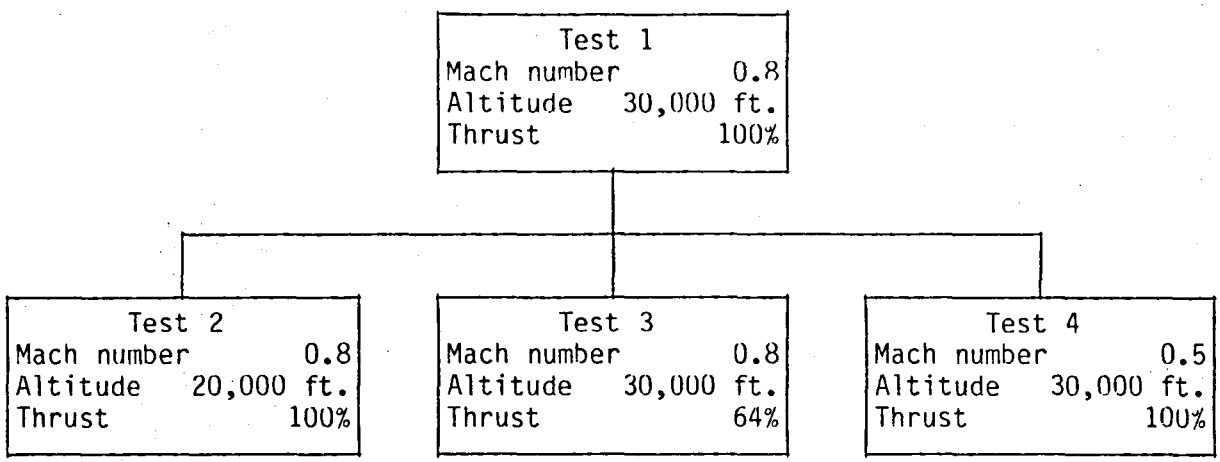

Broadband Shock Noise

The frequency distribution of broadband shock noise is generally quite high throughout the 50 to 12500 hertz frequency range in comparison with other propulsion noise sources. In particular, broadband shock noise of the secondary jet can dominate the entire frequency range and all directivity angles as shown in figures 8, 9 and 10.

Broadband shock noise from the primary jet, on the other hand, is not as prevalent as broadband shock noise from the secondary jet. This is because the jet velocity must be quite high as a result of the high jet temperature for shock noise to occur. Referring to figure 8, which shows the spectra from Test 1 at 90 and 120 degrees, broadband shock noise of the primary jet is comparable with the broadband shock noise from the secondary jet. However, in figures 9, 10 and 11 where the jet velocity is lower, the primary jet broadband shock noise level has been significantly reduced.

Fan Noise

Fan noise is a high frequency noise source consisting of noise radiating from the inlet and noise radiating from the nozzle exit plane. Forward radiated fan noise has three components: broadband noise, discrete tones and combination tones. It is the discrete tone which cause sharp spikes in the fan spectra. These spikes occur at integer multiples of the blade passing frequency as shown in figures 8, 9, 10 and 11. Based on the fan noise model, the broadband and discrete tones components of forward radiated fan noise peak at a directivity angle of 30°. Combination tones peak at 60° to the engine inlet. In the absence of broadband shock noise, forward radiated fan noise can dominate the spectra at 30° as shown in figure 11a.

Aft radiated fan noise consists of two components: broadband and discrete tones. Like forward radiated fan noise, it is the discrete tone which causes a sharp spike in the spectra from 1600 to 12500 hertz. Unlike forward radiated fan noise, however, aft radiated fan noise rarely dominates the spectra as a noise source. This is because other noise sources such as jet mixing noise, turbine noise and broadband shock noise also peak in the aft arc at about 120° to the engine inlet. Never-the-less, aft radiated fan noise does contribute to the OASPL in the high frequency range.

Jet Mixing Noise

Jet mixing noise is a low to moderate frequency noise source which peaks at about 140° to the engine inlet. Based on the results of these tests, jet mixing noise from the primary jet was not a significant source in terms of the frequency distribution. However, jet mixing noise from the secondary jet (fan) is a significant noise source. As shown in figures 11, jet mixing noise from the secondary jet dominates the spectra from 50 to 2500 hertz. Even in the presence of broadband shock noise, jet mixing noise from the secondary jet can contribute to the total noise level as shown in figure 8d.

Turbine Noise

Turbine noise is a high frequency noise source consisting of a broadband component and discrete tones. In these tests, the blade passing frequency of the last turbine stage (which is considered as the primary cause of turbine noise) occurs at the 8000 hertz center frequency. It is at this frequency that turbine noise is most prevalent, as shown in figure 11d. Like jet mixing noise, turbine noise peaks in the aft arc of 120° to the engine inlet. Even though turbine noise is not a dominant noise source in terms of the OASPL, it must be considered as a significant noise source based on the high frequency content of the spectra.

Core Noise

Core noise is a low frequency noise source radiation from the primary nozzle exit plane. The OASPL peaks at a directivity angle of 150° to the engine inlet, and the 1/3 octave band spectra peaks at a frequency of approximately 400 hertz.

Based on the results of these tests, the frequency distribution of this source is not sufficient to be considered a primary noise source.

NOISE SOURCE RANKING

As a result of these predictions, the following source ranking is established. The dominant noise sources are listed in Table 10 as a function of directivity angle. Broadband shock noise of the primary jet and the fan occur at all angles and are the most important sources at flight Mach numbers greater than 0.7. At lower flight Mach numbers of .5 and .6, forward radiated fan noise becomes important in the forward arc while aft radiated fan noise and fan mixing noise are important in the aft arc. In addition to the sources listed in Table 10, turbine noise may be added to the list of important noise sources based on the high frequency content of the one-third octave band spectra.

Jet mixing noise of the primary jet and combustor noise in this model do not appear to be significant noise sources in terms of OASPL or frequency content.

SENSITIVITY STUDY

Broadband shock noise, fan noise and jet mixing of the fan bypass flow have been identified as the dominant noise sources for high bypass turbofan engines based on the Lockheed Near-Field Noise Prediction Program. A sensitivity study of these three noise sources was conducted to determine relative importance of configuration and flight condition input parameters.

Broadband Shock Cell Noise

The parameters which determine the OASPL for broadband shock noise are the jet velocity, the total jet temperature, the flight velocity and the nozzle diameter. The magnitude of the OASPL for broadband is determined by the jet Mach number which is a function of the jet velocity and jet total temperature. To demonstrate the effect of the jet Mach number on the OASPL,

noise predictions were made for a static jet where the jet Mach number varied from 0.9 to 1.25. Since the jet Mach number is the relevant parameter for broadband shock noise predictions, the primary and secondary total temperatures were chosen as 1150°R and 525°R, respectively. The primary and secondary jet velocities were computed using

$$V_j = \sqrt{\frac{\gamma R T_j}{\frac{1}{M_j^2} + \frac{\gamma - 1}{2}}} \tag{12}$$

for each jet Mach number M_j.

Table 11 lists the change in OASPL as a function of the jet Mach number. Figure 12 shows the rate of increase in broadband shock noise as a function of jet Mach number of a stationary jet.

The difference between the primary and secondary broadband shock noise calculations is due to the exit nozzle diameter. The OASPL varies as 20 Log D where D is the ratio of the secondary jet diameter to the primary jet diameter. In this case

$$\Delta dB = 20 \text{ Log } \frac{6.44}{2.75} = 7.39 \text{ dB} \tag{13}$$

The observer location for these calculations is 90° to the jet inlet with a radius of 15 feet at standard day conditions. The same calculations were made with a flight Mach number of 0.8. With an observer angle of 90° and a flight Mach number of 0.8, the emission angle is 36.90° as a result of the coordinate transformation. This results in a convective amplification factor of 17.72 dB and accounts for most of the observed difference in the OASPL for the static case and the flight case. Table 12 lists the OASPL for the primary and secondary jets as a function of jet Mach number with a flight Mach number of 0.8. Figure 13 shows the rate of increase in broadband shock noise as a function of jet Mach number at a flight Mach number of 0.8.

Jet Mixing Noise

Jet mixing noise of the secondary nozzle (or the fan) has also been shown to be an important noise source for turbofan engines. The parameters which determine the jet mixing noise level are the jet total temperature, jet velocity and jet nozzle diameter. The prediction of the jet mixing noise of the secondary jet is identical to that of a primary jet with the exception that an equivalent jet temperature and velocity, given by

$$T_e = \frac{T_p + \frac{\dot{m}_s}{\dot{m}_p} T_s}{1 + \frac{\dot{m}_s}{\dot{m}_p}} \qquad (14)$$

and

$$V_e = \frac{V_p + \frac{\dot{m}_s}{\dot{m}_p} V_s}{1 + \frac{\dot{m}_s}{\dot{m}_p}} \qquad (15)$$

are used rather than the actual jet velocity and total temperature. It is instructive, therefore, to look at the prediction of a circular nozzle over a range of jet velocities, total temperatures and nozzle diameters.

Figure 14 shows the jet mixing noise level as a function of jet velocity for several jet total temperatures and two nozzle diameters. A nozzle diameter of 2.75 feet was chosen since this coincides with the primary nozzle diameter of the model turbofan. Primary jet velocities (of the model high bypass turbofan) varied from 1500 feet/sec to 2000 feet/sec while jet total temperatures varied from 1100°R to 1200°R. It can be seen from figure 14 that jet mixing noise level increases significantly with jet velocity. The jet total temperature is most important at V_j = 2000 feet/sec, and becomes less significant as the jet velocity is decreased. Note the 10 dB difference in the noise level at V_j = 2000 feet/sec between T_j = 1000°R and 2000°R as compared to almost no difference in the noise level with jet total temperature at V_j = 1250 feet/sec.

In contrast, with a nozzle diameter of 7.0 feet (which coincides with the nozzle diameter of the secondary jet), jet velocity is the parameter which determines the noise level with temperature effects being almost insignificant. The difference in the noise level between D_j = 2.75 and D_j = 7.0 for V_j = 1250 feet/sec points out the importance of the nozzle diameter as an input parameter.

Noise sources such as the fan, turbine, core, and broadband shock are considered to be point sources which move with the engine. Jet mixing noise, on the other hand, is a distribution of sources which move in the jet mixing region. The motion of these sources is built into the prediction model and,

therefore, does not require a correction for convective amplification. It is interesting to compare the noise level of a stationary jet and a jet in flight since the effect of flight on jet mixing noise is exactly opposite of the effect of convective amplification for point sources.

Figure 15 shows the jet mixing noise level plotted as a function of the observer angle ϕ for a stationary jet and a jet flying at Mach 0.8. The noise level of the static jet is considerably higher (19.0 dB at $\phi = 30°$) than the noise level at $M_f = 0.8$. This trend holds for all observer angles, and, in fact, the difference is greater for $\phi < 90°$ than for $\phi > 90$.

Fan Noise

Fan noise is the remaining noise to be studied which has been shown to be an important propulsion noise source. Three flight condition parameters determine the fan noise level, the mass flow rate $\dot{m}$, the temperature rise across the fan ΔT, and the rotation speed N. The sensitivity of the fan noise level to mass flow rate and temperature rise ΔT are given directly by the following equations:

$$\Delta dB_{\dot{m}} = 10 \text{ Log } \frac{\dot{m}}{\dot{m}_{ref}} \tag{16}$$

where

$$\dot{m}_{ref} = \begin{cases} 142.9 \text{ kg/sec} \\ 315.0 \text{ lbm/sec} \\ 9.79 \text{ slug/sec} \end{cases} \tag{17}$$

and

$$\Delta dB_{\Delta T} = 20 \text{ Log } \frac{\Delta T}{\Delta T_{ref}} \tag{18}$$

where

$$\Delta T_{ref} = \begin{cases} 44.4 \text{ °K} \\ \text{or} \\ 80° \text{ °R} \end{cases} \tag{19}$$

The noise levels given by rotational speed variation is more complex since the rotational speed N is only one parameter in the expression for the relative tip Mach number which is the parameter used to correlate noise level fluctuation. (For more detail see Appendix C). In general, variations in rotational speed have minimal impact on the fan noise level.

CONCLUSIONS

This study has investigated the near-field noise prediction capability of the Lockhead Near-Field Noise Prediction Program. Estimated full scale performance data for a high bypass turbofan engine were obtained to determine changes in the OASPL of propulsion noise sources due to variations in altitude, thrust and flight Mach number. Based on results from the Lockheed program, the dominant propulsion noise sources during cruise were identified as broadband shock noise of the primary and secondary jets, jet mixing noise of the secondary jet, and fan noise. Broadband shock noise is the single most important source during cruise since it was always present in the secondary jet.

This study also examines the sensitivity of the OASPL of the three dominant sources to variations in the flight input parameters. The conclusions are:

For broadband shock noise:

- Broadband shock noise occurs when the jet Mach number is greater than one and increases rapidly as the jet Mach number increases. To calculate the jet Mach number requires an accurate knowledge of the jet velocity and jet total temperature.

- Broadband shock noise can be expected in the secondary flow of a high bypass turbofan during cruise. This is the result of a relatively low jet total temperature causing the jet Mach number to be typically greater than one.

For jet mixing noise:

- The jet mixing noise OASPL is determined by three parameters: the jet velocity, the jet total temperature and the nozzle diameter.

- In the near-field, the jet mixing noise increased approximately as V^N where N is between 5 and 7. This is somewhat lower than the V^8 law attributed to far-field jet mixing noise.

- Temperature effects were found to be negligible in the secondary jet with the noise level varying only 1.5 dB with a 500° increase in the jet total temperature.

- The OASPL of the secondary flow will increase as the nozzle diameter increases. However, unlike the primary jet nozzle where the nozzle diameter can vary during cruise, the secondary nozzle diameter is fixed and therefore does not contribute to an increase or decrease in the secondary jet mixing noise level.

For fan noise:

- Fan mean square pressure increases as the square of the temperature rise across the fan and linearly with the mass flow rate through the

fan. During cruise, the mass flow rate can be expected to vary significantly with altitude variation. The temperature rise across the fan, on the other hand, will vary only a few degrees and, therefore, not contribute to fan noise fluctuations during cruise.

- Variations in the rotational speed of the fan will change the fan blade passing frequency. If the blade passing frequency is on the dividing line between two one-third octave bands, an increase (or decrease) in the rotational speed may cause a discrete tone to pass over into an adjacent third octave thus changing the character of the spectra. This is a special case, however. Generally variations in the rotational speed will have negligible impact on the OASPL and one-third octave band spectra.

These conclusions are based on the ability to accurately predict noise levels in flight. The major concern for noise predictions during cruise are not the empirical algorithms but the modifications for altitude and flight effects. Based on the poor agreement with flight data, J. Tibbet (ref. 1) suggests a correction for altitude of 20 log $\rho c^2/\rho_0 c_0^2$. If this is the case, it would not change the conclusions of this study, since an altitude correction would be applied to each noise source and the relative level between sources would not change.

What would change the conclusions of this study, however, would be the corrections for flight effects. It seems inconsistent that jet mixing noise should decrease in flight at all directivity angles while the remaining propulsion noise sources increase in OASPL in the forward arc and decrease in the aft arc. If either of these observations is incorrect then jet mixing noise of the primary jet may become a dominant source. If the convective amplification factor of -40 log (1. - M_a cos ϕ) is incorrect, as has been suggested for broadband shock noise by C. Tam (ref. 8), then broadband shock noise may not be the most dominant source.

The Lockheed Near-Field Noise Prediction Program is a convenient program for making qualitative estimates of the near-field noise environment of an aircraft in cruise. The technology base of the program is valid for sea level noise predictions. Modifications for cruising altitude and flight speed in the Mach 0.8 range are needed. The following modifications to the program are suggested based on techniques developed since the program release in 1979.

The first concerns the convective amplification factor for broadband shock noise. The work of C. Tam (ref. 8) indicates the convective amplification factor for broadband shock noise should be

$$CA_{NEW} = 20 \text{ Log } \left(\frac{\alpha}{1 - M_a \cos \phi'}\right) \quad ; \quad \phi' < 90° \tag{20}$$

rather than

$$CA = 40 \text{ Log}(1/(1 - M_a \cos \phi')) \tag{21}$$

expression. The stretching factor α is the ratio of the potential core length of a jet in flight to that of a stationary jet, i.e.,

$$\alpha = \frac{L_f}{L_s} \tag{22}$$

Michalke and Michel (ref. 9) give an estimate for the stretching factor α as

$$\alpha = 1 - A \frac{V_a}{V_j - V_a} \tag{23}$$

where the stretching parameter A is

$$1.5 \leq A \leq 3. \tag{24}$$

If A is set to 2 as suggested by Michalke and Michel, then the convective amplification factor for $M_f = 0.8$ at 30° would be 16.23 dB rather than 20.50 dB predicted by equation 20. This is still a substantial increase in the noise level in the forward arc ($\phi < 90°$), but there is less of an increase than with the original convective amplification factor.

One limitation to using this method is that the emission angle must be less than 90°. However, at $M_f = 0.8$ an emission angle of 90° corresponds to an observer angle of 129°, which covers most of the region of interest for near-field predictions.

A second modification is also suggested to the broadband shock noise prediction method. The SAE broadband shock noise prediction method is based on the same method used in the Lockheed program with a correction for heated and unheated jets. This would require modifying the exponent ℓ of the shock parameter β as follows:

$$\ell = \begin{cases} 4 & \beta \leq 1 \quad \text{all jets} \\ 2 & \beta > 1 \quad \text{heated jets} \\ 1 & \beta > 1 \quad \text{unheated jets} \end{cases} \tag{25}$$

(Refer to Appendix A for details on broadband shock noise predictions.) A heated jet is defined as a jet with a total to static temperature ratio greater than 1.1. This will reduce the noise level of unheated jets. This would not change the results of the broadband shock noise predictions in this study since the shock parameter β was always less than 1. However, this may not be true for all turbofan engines.

A third modification is suggested to the jet mixing noise prediction method for coaxial nozzle engines. The bypass ratio and area ratio should be included as a flight condition parameter since this would more accurately represent the operation of a turbofan engine.

A modification to the fan noise prediction method would be to eliminate the relative tip Mach number M_{T_R} as an input and replace it with the fan

blade length b. The relative tip Mach number can then be computed internally as indicated by equation C6. This will ensure that changes in rotational speed and mass flow are accurately reflected in the relative tip Mach number.

Finally, a modification to the observer coordinate input would include a third dimension z, so that the distance from source to observer will be given by

$$r = \sqrt{x^2 + y^2 + z^2} \tag{26}$$

This will account for variations in the location of the engine nozzle relative to a wing surface rather than assuming they both lie in the same plane.

Appendix A

A1. Broadband Shock Noise

Jet broadband shock noise occurs when the pressure ratio in the jet exhaust nozzle is supercritical causing shock cells to form and expand in the jet mixing region. The method used to predict broadband shock noise was developed by Harper-Bourne and Fisher (ref. 10) with modifications to include forward flight effects. The dynamic effect has been removed from the broadband shock noise prediction code since Swift and Mugur indicate (ref. 3) that it is appropriate only for distributed noise sources such as jet mixing noise.

The acoustic mean square pressure for broadband shock noise is given by

$$\frac{p^2}{p_{ref}^2} = \beta^{\ell} \frac{|(1 + G)|}{(r'/D_e)^2} \frac{W_1 f_i (10^{H_i/10})(\rho_a c_a/\rho_0 c_0)}{(1 - M_a \cos \phi')^4} \tag{A1}$$

Shock cells form when the strength parameter β, defined as

$$\beta = \sqrt{M_j^2 - 1.0} \tag{A2}$$

is greater than 1. The jet Mach number M_j is given as a function of the jet velocity V_j and jet total temperature T_j by

$$M_j = \left[\frac{\gamma R T_j}{V_j^2} - \left(\frac{\gamma - 1}{2}\right)\right]^{-1/2} \tag{A3}$$

For the primary jet, the ratio of specific heat γ is taken as 1.33, and for the secondary jet γ is 1.4.

The acoustic mean square pressure is proportional to β raised to the power ℓ where ℓ is given for two regions by

$$\ell = \begin{cases} 4 & \text{if} \quad \beta \leq 1.0 \quad \text{or} \quad M_j \leq \sqrt{2} \\ 2 & \text{if} \quad \beta > 1.0 \quad \text{or} \quad M_j > \sqrt{2} \end{cases} \tag{A4}$$

For most high-bypass turbofans the β^4 relation will hold since jet Mach numbers during cruise tend to be less than $\sqrt{2}$.

The propagation distance r' defined by equation 3 is normalized by the equivalent nozzle diameter D_e. The equivalent nozzle diameter is calculated from the nozzle exit area by

$$D_e = \sqrt{\frac{4A}{\pi}} \tag{A5}$$

In the case of a single circular jet without a plug, the equivalent jet diameter is equal to the nozzle jet diameter. In the case of a nozzle with a plug or a secondary jet, the area of the nozzle should exclude the area of the plug or the area of the primary jet.

Broadband shock noise is assumed to occur for shock cells distributed along the centerline of the nozzle. The spacing of the first shock cell intersection from the nozzle lip is given by

$$L_1 = K_1 H_j \beta \tag{A6}$$

where K_1 is a spacing constant given by

$$K_1 = 1.31 \tag{A7}$$

and H_j is a characteristic length determined by the type of nozzle. For a circular jet with or without a plug

$$H_j = D_e \tag{A8}$$

For a secondary nozzle H_j is annulus height. The average spacing of the remaining shock cells is

$$L_a = K_0 H_j \beta \tag{A9}$$

where K_0 is the average spacing constant given by

$$K_0 = 1.10 \tag{A10}$$

The source interference function $|1 + G|$ is defined in terms of the empirical function G given by

$$G = \frac{4}{N_s \cdot b_c \cdot w_i} \sum_{n=1}^{N_s-1} \left[C_i^{n^2} \sum_{s=1}^{N_s-n} \frac{\cos(W_c \cdot Q_{ns}) \sin(b_c \omega_i Q_{ns}/2.0)}{Q_{ns}} \right] \tag{A11}$$

The summation in G is taken over 8 shock cells so that

$$N_s = 8 \ . \tag{A12}$$

The remaining parameters required to compute G are defined below:

$b_c = 0.2316$	one-third octave band center frequency bandwidth constant
$\omega_i = 2\pi f_i$	one-third octave band angular frequency
f_i	one-third octave band center frequencies
i	index on one-third octave band center frequencies $i = 1, \ldots, 24$
c_i	correlation coefficient given in table A1 as a function of the Strouhal number σ_i
$\sigma_i = \frac{\omega_i L_0}{c_a}$	Strouhal number
c_a	ambient sound speed
$W_2 = L_1 D_F V_c$	empirical coefficient
$D_f = 1 - M_c \cos(180° - \phi')$	Doppler factor
$M_c = V_c/c_a$	eddy convection Mach number
$V_c = CV_j$	eddy convection velocity
$C = 0.70$	eddy convection velocity constant

The source spectral distribution is given by the function H_i given in Table A1. The spectra distribution amplitude W_1 is given by

$$W_1 = \frac{2\pi b_c D_e \beta}{c_a} \tag{A13}$$

The terms $\rho_a c_a/\rho_0 c_0$ and $(1 - M \cos \phi')^4$ account for the acoustic impedance correction and convective amplification, respectively.

Appendix B

JET MIXING NOISE

The method used to predict jet mixing noise in the Lockheed Near-Field Noise Prediction Program was developed by Plumbees (ref. 11). Modifications to the method were made by Lockheed to include co-axial nozzle and forward flight effects. These modifications include the cruise coordinate transformation and dynamic amplification. A brief discussion of the circular jet prediction method is given followed by a description of the modification for a coaxial jet nozzle.

Primary Jet

The mean square acoustic pressure of a simple circular nozzle is predicted for three octave band and the overall by

$$\frac{\overline{p}^2(I)}{p_{ref}} = \frac{1}{C_{10}} [A(I,17)\ C_9 (\frac{T_j}{T_{ref}})^{1.54} M^4\ (1 + \cos^4\theta)][\frac{C_1}{r^2} + \frac{C_2}{r^4} + \frac{C_3}{r^6}] \quad (B1)$$

Turbulent eddies are assumed to be convected downstream at a Mach number M given by

$$M = M_j\ [1 - \frac{V_A}{V_j}]^{3/4} \quad (B2)$$

The coefficients C_1, C_2, C_3, C_6 and C_7, which are functions of jet total temperature T_j and convected Mach number, M, are given by

$$C_1 = M^{2.34} \quad (B3)$$

$$C_2 = 10.65\ (T_J/t_a)^{0.93} \quad (B4)$$

$$C_3 = -15.18\ (T_J/t_a)^{1.11}\ M^{0.89} \quad (B5)$$

$$C_6 = 17.5\ (T_J/3T_{ref})^{0.89(M^2 - 1)} \quad (B6)$$

$$C_7 = 0.41\ (T_J/3.6T_{ref})^{0.566(M^2 - 1)} \quad (B7)$$

where t_a is the ambient temperature, and the reference temperature T_{ref} i defined as

$$T_{ref} = \begin{cases} 555.6\ °K \\ 1000.0\ °R \end{cases} \quad (B8)$$

The coefficients α, C_4, C_5, C_9 and C_{10}, which are functions of total jet temperature, convected Mach number and frequency, are given by

$$\alpha^2 = A(I,1)M^{A(I,2)}(T_J/T_{ref})^{A(I,3)} + A(I,4)M \tag{B9}$$

$$C_4 = A(I,5)M^{A(I,6)}(T_J/T_{ref})^{A(I,7)} + A(I,8)M \tag{B10}$$

$$C_5 = A(I,9)M^{A(I,10)}(T_J/T_{ref})^{A(I,11)} + A(I,12)M \tag{B11}$$

$$C_9 = \left[\frac{(1 + \alpha^2M^2)}{\alpha^2M^2 + \left(1 - \frac{M\cos\theta}{1 + C_6e^{-C_7r}}\right)^2}\right]^{5/2} \tag{B12}$$

$$C_{10} = 1 + \frac{C_4e^{-C_5\theta}}{1 + C_6e^{-C_7r/4}} \tag{B13}$$

The coefficient matrix $A(I,J)$, $I = 1$ to 4 and $J = 1$ to 17, is given in Table B1.

The propagation distance r and emission angle θ for a stationary jet are given as a function of the normalized source coordinates $(\bar{x}_0, \bar{y}_0)$ and the normalized observer coordinates $(\bar{x}, \bar{y})$

Two cases are considered for the computation of r and θ. First, if the $\bar{y}$ component of the observer is greater than the y component of the source, i.e., when

$$\bar{y} > \bar{y}_0(I) \tag{B14}$$

then

$$r = r_s(I) = \sqrt{(\bar{x} - \bar{x}_0(I))^2 + \bar{y} - \bar{y}_0(I))^2} \tag{B15}$$

and

$$\theta = \theta_s(I) = \tan^{-1}\left[\frac{\bar{y} - \bar{y}_0(I)}{\bar{x} - \bar{x}_0(I)}\right] \tag{B16}$$

If the y component of the observer is less than the y component of the source and the observer is upstream of the nozzle exit plane, i.e.,

$$\bar{y} \leq \bar{y}_0 \tag{B17}$$

and

$$\bar{x} < 0 \tag{B18}$$

then

$$r = r_s(I) = \sqrt{(\bar{x} - \bar{x}_0(I))^2 + \bar{y}^2} \tag{B19}$$

and

$$\theta = \theta_s(I) = 180° \tag{B20}$$

Figure 17 shows the source/receiver geometry for jet mixing noise. The source coordinates $\bar{x}_0(I)$ and $\bar{y}_0(I)$, which also define the shear layer boundary, are given as a function of the jet total temperature, convected Mach number and frequency by

$$x_0(I) = A(I,13)M^{A(I,14)}\ (T_J/T_{ref})^{A(I,15)} + A(I,16)M \tag{B21}$$

$$y_0(I) = 0.5 + 0.132\ x_0(I) \tag{B22}$$

The normalized observer coordinates x and y are given by

$$\bar{x} = x/D_j \tag{B23}$$

and

$$\bar{y} = y/D_j \tag{B24}$$

where x and y are the physical observer coordinates and D_j is the jet nozzle diameter.

In flight the propagation distance $\bar{r}_s'(I)$ and emission angle $\theta_s'(I)$ are given as a function of the stationary coordinates r and θ. Again, two cases are considered. When

$$\bar{y} \leq \bar{y}_0$$

then

$$\theta_s'(I) = \cot^{-1}\left[\frac{1}{1 - M_A^2}\left(\cot\theta_s(I) - M_A\sqrt{1 - M_A^2 + \cot^2\theta_s(I)}\right)\right] \quad (B25)$$

and

$$\bar{r}_s'(I) = \frac{\bar{y} - \bar{y}_0(I)}{\sin\theta_s'(I)} \quad (B26)$$

When

$$\bar{y} > \bar{y}_0(I) \quad (B27)$$

and

$$\bar{x} < 0 \quad (B28)$$

then

$$\theta_s'(I) = 180° \quad (B29)$$

and

$$\bar{r}_s'(I) = \bar{r}_s(I)/(1.0 - M_A) \quad (B30)$$

The angle θ_s' must be greater than 7.5° which is the slope of the jet spear layer. This restricts an observer from being in the mixing region of the jet.

The Sound Pressure Level for the overall and the three octave bands is given by

$$SPL(I) = 10\ \text{Log}\ \frac{\bar{p}^2(I)}{p_{ref}^2} \qquad I = 1, 2, 3, 4 \quad (B31)$$

Now that the jet mixing noise has been computed for the overall and the three octave bands, the frequency range is expanded to cover frequencies from 50 to 10,000 Hz. For frequencies less than F(2) > 50 Hz where

$$F(I) = \frac{H_N(I)c_a}{D_j} \qquad I = 1, 2, 3, 4 \quad (B32)$$

and $H_N(I)$ is the Hemholtz number given in Table B2, the reduced Sound Pressure Level is given by

$$SPL_A(N) = SPL(2) - L_A(N) + L_A(2) \qquad N = 2, 4, 8, \ldots \quad (B33)$$

The term $L_A(N)$ is given in Table B3 as a function of the Strouhal number $S_A(N)$ where

$$S_A(N) = \frac{0.221\ c_a F_A(N)}{V_j\ F(2)} \quad (B34)$$

and

$$F_A(N) = \frac{F(2)}{N} \quad (B35)$$

Equations B33, B34 and B35 are repeated until

$$F_A(N) > 50 \text{ Hz} \quad (B36)$$

Similarly, for frequencies above $F(4) < 10{,}000$ Hz,

$$SPL_B(N) = SPL(4) - L_B(N) + L_B(2) \qquad N = 2, 4, 8 \quad (B37)$$

The term $L_{B_N}(\overline{x})$ (also given in Table B3) is given as a function of the Strouhal number $S_B(N)$ where $S_B(N)$ is defined by

$$S_B(N) = \frac{0.884\ c_a}{V_j} \frac{F_B(N)}{F(4)} \quad (B38)$$

and

$$F_B(N) = N \cdot F(4) \quad (B39)$$

Equations B37, B38 and B39 are repeated until

$$F_B(N) \geq 10{,}000 \text{ Hz}. \quad (B40)$$

Octave band levels are obtained for each one-third octave band center frequency f_i by interpolating SPL(I) and log F(I) in the $\log(f_i)$. This gives the octave band level at each one-third octave band center frequency. These octave band levels are converted to free-field one-third octave band levels by

$$SPL_i(1/3\ O.B.L.) = SPL_i(O.B.L.) - 4.85 \quad (B41)$$

Equation B41 gives the freefield SPL for the 24 one-third octave band center frequencies from 50 to 10,000 Hz for a circular jet nozzle in flight. The freefield SPL is corrected for the local acoustic impedance and dynamic amplification by

$$SPL_i = SPL_{i_{freefield}} + 10 \text{ Log } \left(\frac{p_a c_a}{p_o c_o}\right) + 10 \text{ Log } \left(\frac{1}{1 - M_a \cos \phi'}\right); \; i = 1,\ldots,24 \tag{B42}$$

where

$$\phi' = \pi - \theta' \tag{B43}$$

and i is the index on the one-third octave band center frequencies.

Circular Jet with Plug Nozzles

The prediction of jet mixing noise for primary jets with plugs requires two modifications. First, the observer coordinates x and y are normalized by the equivalent jet diameter D_e given by

$$D_e = 2H\sqrt{H(D_j - H)} \tag{B44}$$

where D_j is the jet diameter and H is the annular height as shown in figure B2. The normalized observer coordinates then become

$$\overline{x} = \frac{x}{D_e} \tag{B45}$$

and

$$\overline{y} = \frac{y}{D_e} \tag{B46}$$

which are then used in place of equation B23 and B24.

The second modification is to adjust the octave band SPL and the frequency for the presence of the plug by

$$SPL(I) = 10 \log \frac{\overline{p^2}(I)}{p^2_{ref}} + 3 \log(0.10 + 2H/D_e) \tag{B47}$$

and

$$F(I) = \frac{H_N(I)c_a}{D_e R_d^{0.4}} \tag{B48}$$

where the Strouhal number correction parameter R_d is given by

$$R_d = 2(H/D_e) \tag{B49}$$

Secondary Jet

The prediction of jet mixing noise for coaxial jets is achieved by calculating an equivalent jet total temperature, jet velocity and Mach number and, in essence, repeating the calculation as a circular jet. The equivalent jet total temperature is given by

$$T_e = \frac{T_j + \frac{\dot{m}_s}{\dot{m}_p} T_s}{(1 + \frac{\dot{m}_s}{\dot{m}_p})} \tag{B50}$$

quivalent jet velocity by

$$V_e = \frac{V_j + \frac{\dot{m}_s}{\dot{m}_p} V_s}{(1 + \frac{\dot{m}_s}{\dot{m}_p})} \tag{B51}$$

The equivalent jet Mach number for a stationary nozzle is given by

$$M_e = \frac{V_e}{\sqrt{\gamma R(T_e - \frac{V_e^2}{2c_p})}} \tag{B52}$$

and in flight the equivalent jet Mach number is given by

$$M_e = \frac{V_e\left(1 - \frac{V_A}{V_e}\right)^{.25}}{\sqrt{\gamma R\left(T_e - \frac{V_e^2}{2c_p}\right)}} \tag{B53}$$

The octave band SPL for the secondary jet is obtained by substituting M_e for M, T_e for T_j, V_e for V_j and D_s for D_j and repeating the calculation for a circular jet.

The total SPL of the coaxial jet due to jet mixing noise is given by

$$SPL_{TOTAL}^{(I)} = 10\ Log^{SPL_1^{(I)}} + 10\ Log^{SPL_2^{(I)}} \tag{B54}$$

where SPL_1 is the SPL of the primary jet and SPL_2 is the SPL of the secondary jet. Before equation B54 can be computed, however, the SPL of the primary jet must be corrected for the presence of the secondary jet by

$$\Delta SPL = 10\ M_c\ \log\left(1 - \frac{V_A}{V_j}\right)^{3/4} \tag{B55}$$

so that

$$SPL_1^{(I)} = SPL_{(Primary)}^{(I)} + \Delta SPL\ . \tag{B56}$$

The correction factor M_c is given in Table B4 as a function of the Strouhal number and area ratio between the secondary jet and the primary jet.

Appendix C

FAN NOISE

The fan noise source algorithm is based on the method of M. F. Heidman (ref. 12). The prediction of fan noise is divided into two parts: noise radiating from the fan inlet and noise radiating from the nozzle exit plane. Inlet radiated noise has three components, broadband noise, discrete tone noise and combination tones. Broadband noise and discrete tone noise are always present while combination tones occur only when the relative tip Mach number is greater than one. Fan noise radiating from the nozzle exit plane consists of broadband noise and discrete tone noise.

The general form of the mean square pressure for fan noise is given by

$$\frac{\overline{p}^2}{p_{ref}^2} = \left[\frac{K(\rho_a c_a/\rho_0 c_0)}{(r'/r_{ref})^2(1-M_A\cos\phi')^4}\left(\frac{\Delta T}{\Delta T_{ref}}\right)^2\left(\frac{\dot{m}}{\dot{m}_{ref}}\right)\right]\left[\frac{G(M_{T_R},(M_{T_R})_D)I(IGV)D(\phi')S(n)}{H(RSS)}\right] \tag{C1}$$

The terms in the first set of brackets,

$$\frac{K(\rho_a c_a/\rho_0 c_0)}{(r'/r_{ref})^2(1-M_A\cos\phi')^4}\left(\frac{\Delta T}{\Delta T_{ref}}\right)^2\left(\frac{\dot{m}}{\dot{m}_{ref}}\right) \tag{C2}$$

are common to all five components of fan noise. The correction for the local impedance is given by $(\rho_a c_a/\rho_0 c_0)$, the correction for convective amplification is given by $(1 - M_A \cos\phi')^4$, and the constant K is defined as

$$K = 10^{6.3} \tag{C3}$$

The two terms which are most important in determining the fan noise sound pressure level are ΔT, the temperature rise across the fan stage, and $\dot{m}$, the mass flow rate through the fan. The reference parameter ΔT_{ref} and $\dot{m}_{ref}$ are given by

$$\Delta T_{ref} = \begin{cases} 44.4\ ^\circ K \\ \text{or} \\ 80^\circ\ ^\circ R \end{cases} \tag{C4}$$

and

$$\dot{m}_{ref} = \begin{cases} 142.9 & \text{kg/sec} \\ 315 & \text{lbm/sec} \\ 9.79 & \text{slugs/sec} \end{cases} \tag{C5}$$

The emission angle ϕ' and the propagation distance r' defined by equation 2 and 3, respectively, are different for fan noise radiating from the inlet and the discharge as shown in figure 18. This is accomplished by a simple coordinate transformation.

The functions G, H and I and the spectrum function $S(\eta)$ in the second set of brackets are described below for each of the five fan noise components. The directivity function $D(\phi')$ for the five fan noise components is given in Table C1.

Inlet Broadband Fan Noise

The arguments of the function $G(M_{T_R}, (M_{T_R})_D)\, M_{T_R}$, are the relative tip Mach number M_{T_R} and the relative tip Mach number at the design point $(M_{T_R})_D$. The relative tip Mach number is defined as

$$M_{T_R}^2 = M_T^2 + M_X^2 \tag{C6}$$

where M_T is the tip Mach number given by

$$M_T = \frac{2\pi Nb}{60\ c_a} \tag{C7}$$

N = rotational speed in RPM
b = fan blade length
c_a = ambient speed of sound

and M_X is the axial Mach number given by

$$M_X = \frac{\dot{m}}{\rho_a c_a A} \tag{C8}$$

$\dot{m}$ = fan mass flow rate
ρ_a = ambient density
c_a = ambient speed of sound
A^a = fan inlet area

The function G for inlet broadband fan noise is

$$10\text{Log}G(M_{T_R},(M_{T_R})_D) = \begin{cases} 58 & \text{for } M_{T_R} \leq 0.9 \text{ and } (M_{T_R})_D \leq 1.0 \\ 58 + 20\ \text{Log}(M_{T_R})_D & \text{for } M_{T_R} \leq 0.9 \text{ and } (M_{T_R})_D > 1.0 \\ 57.6 - 20\ \text{Log}(M_{T_R}) & \text{for } M_{T_R} > 0.9 \text{ and } (M_{T_R})_D < 1.0 \\ 57.6 + 20\ \text{Log}[(M_{T_R})_D/M_{T_R}] & \text{for } M_{T_R} > 0.9 \text{ and } (M_{T_R})_D \geq 1.0 \end{cases} \quad \text{(C9)}$$

The correction for rotor stator spacing function H(RSS) is given by

$$H(RSS) = \sqrt{RSS/300} \quad \text{(C10)}$$

where the rotor stator spacing is defined in figure 19.

Since no correction is required for the presence of inlet guide vanes, the function I(IGV) is unity.

$$I(IGV) = 1. \quad \text{(C11)}$$

Finally, the spectrum function S(n) is given by

$$S(n) = \exp[-4.264(\text{Log } n_i)^2] \quad \text{(C12)}$$

where the frequency parameter for broadband fan noise is given by

$$n_i = f_i/f_{ref} \quad \text{(C13)}$$

f_i = one-third octave band center frequency

f_{ref} = one-third octave band center frequency containing 2.5 x BPF (C14)

$$\text{BPF} = N \cdot \frac{N_R}{60} \text{ Blade Passing Frequency} \quad \text{(C15)}$$

N = rotational speed in rev/min

N_R = number of rotor blades

Inlet Discrete Tone Fan Noise

The function G for inlet discrete tone fan noise is given by

$$10 \text{ Log } G(M_{T_R},(M_{T_R})_D) = \begin{cases} 60.5 & \text{for } M_{T_R} \leq 0.72 \text{ and } (M_{T_R})_D \leq 1.0 \\ 60.5 + 20 \text{ Log}(M_{T_R})_D & \text{for } M_{T_R} \leq 0.72 \text{ and } (M_{T_R})_D > 1.0 \\ \min(g_1,g_2) & \text{for } M_{T_R} > 0.72 \text{ and } (M_{T_R})_D < 1.0 \\ \min(g_3,g_4) & \text{for } M_{T_R} > 0.72 \text{ and } (M_{T_R})_D \geq 1.0 \end{cases} \quad \text{(C16)}$$

where

$$g_1 = 60.5 + 50 \text{ Log } (M_{T_R}/0.72) \quad \text{(C17)}$$

$$g_2 = 59.5 - 80 \text{ Log } (M_{T_R}) \quad \text{(C18)}$$

$$g_3 = 60.5 + 20 \text{ Log } (M_{T_R})_D + 50 \text{ Log } (M_{T_R}/0.72) \quad \text{(C19)}$$

and

$$g_4 = 59.5 + 80 \text{ Log } [(M_{T_R})_D/M_{T_R}] \quad \text{(C20)}$$

The definition of $\min(g_1,g_2)$ is the minimum value of the two function g_1 and g_2.

The spectrum function for discrete tone $S(n)$ is given in integer multiples of the blade passing frequency defined by

$$n_i = k \cdot BPF \quad \text{(C21)}$$

and, as a function, the tone cutoff factor is defined by

$$\delta = \left| \frac{M_T}{1 - \frac{N_s}{N_R}} \right| \quad \text{(C22)}$$

where

M_T = Tip Mach number
N_s = number of rotor stators
N_r = number of rotor blades

The first harmonic of the spectrum function $S(n)$ is given by

$$10 \text{ Log } S(n_1) = \begin{cases} 0 & \text{for} \quad \delta > 1.05 \\ \\ -8.0 & \text{for} \quad \delta < 1.05 \end{cases} \tag{C23}$$

Higher harmonics depend on the presence of inlet guide vanes. Without inlet guide vanes:

$$10 \text{ Log } S(n_k) = 3(1 - k) \qquad k = 2, 3, \ldots \tag{C24}$$

and with inlet guide vanes

$$10 \text{ Log } S(n_k) = -3(1 + k) \qquad k = 2, 3, \ldots \tag{C25}$$

The level is assigned to the one-third octave band containing the harmonic frequency.

Since the blade passing frequency and its integer multiples are not in general equal to the one-third octave band center frequencies, the tone level is assigned to the one-third octave band containing the harmonic frequency.

Inlet Combination Tones

Inlet combination tones occur only when the relative tip Mach number is supersonic. They are the result of shock waves forming on the leading edge of each rotor blade and propagating through the inlet duct. Three sound pressure levels are computed corresponding to one-half, one-fourth and one-eighth the fundamental blade passing frequency. The total sound pressure level of the combination tones is obtained by summing the three contributions as

$$SPL = 10^{SPL_{1/2}/10} + 10^{SPL_{1/4}/10} + 10^{SPL_{1/8}/10} \tag{C26}$$

The relative tip Mach number dependence for the three inlet combination tones are given by

$f/f_b = 1/2$

$$G(M_{T_R}, (M_{T_R})_D) = \begin{cases} 785.68 \log(M_{T_R}) + 30.0 & M_{T_R} \leq 1.146 \\ \\ -49.62 \log(M_{T_R}) + 79.44 & M_{T_R} > 1.146 \end{cases} \tag{C27}$$

$f/f_b = 1/4$

$$G(M_{T_R},(M_{T_R})_D) = \begin{cases} 391.81 \log(M_{T_R}) + 30.0 & M_{T_R} \leq 1.322 \\ -50.06 \log(M_{T_R}) + 83.57 & M_{T_R} > 1.322 \end{cases} \quad (C28)$$

$f/f_b = 1/8$

$$G(M_{T_R},(M_{T_R})_D) = \begin{cases} 199.20 \log(M_{T_R}) + 30.0 & M_{T_R} \leq 1.610 \\ -49.89 \log(M_{T_R}) + 81.52 & M_{T_R} > 1.610 \end{cases} \quad (C29)$$

When inlet guide vanes are present the sound pressure level is reduced by 5 dB as indicated by the function I(IGV)

$$10 \text{ Log } I(IGV) = \begin{cases} 0 & \text{without inlet guide vanes} \\ -5 & \text{with inlet guide vanes} \end{cases} \quad (C30)$$

Spectra functions for the three subharmonic tones are given by

$f/f_b = 1/2$

$$n_i = f_i/f_b \quad (C31)$$

$$10 \text{ Log } S(n_i) = \begin{cases} 30 \text{ Log } n_i + 9.03 & n_i \leq 0.5 \\ -30 \text{ Log } n_i - 9.03 & n_i > 0.5 \end{cases} \quad (C32)$$

$f/f_b = 1/4$

$$10 \text{ Log } S(n_i) = \begin{cases} 50 \text{ Log } n_i + 30.1 & n_i = 0.25 \\ -50 \text{ Log } n_i - 30.1 & n_i = 0.25 \end{cases} \quad (C33)$$

$f/f_b = 1/8$

$$10 \text{ Log } S(n_i) = \begin{cases} 50 \text{ Log } n_i + 45.15 & n_i \leq .125 \\ -30 \text{ Log } n_i - 27.09 & n_i > .125 \end{cases} \quad (C34)$$

Discharge Broadband Fan Noise

The relative tip Mach number dependence for the broadband fan noise from the discharge duct is given by

$$10 \text{ Log } G(M_{T_R}, (M_{T_R})_D) = \begin{cases} 60 & \text{for } (M_{T_R})_D > 1.0 \text{ and } M_{T_R} \leq 1.0 \\ 60 + 20 \text{ Log}(M_{T_R})_D & \text{for } (M_{T_R})_D \leq 1.0 \text{ and } M_{T_R} > 1.0 \\ 60 + 20 \text{ Log}[(M_{T_R})_D / M_{T_R}) & \text{for } (M_{T_R})_D > 1.0 \end{cases} \quad \text{(C35)}$$

The correction for rotor stator spacing, H(RSS) the flow distortion function I(IGV) and the spectrum function are identical to the inlet broadband function described for inlet broadband noise.

Discharge Discrete Tone Fan Noise

The relative tip Mach number dependence for the discrete tones from the fan discharge duct are

$$10 \text{ Log } G(M_{T_R}, (M_{T_R})_D) = \begin{cases} 63.0 & \text{for } M_{T_R} \leq 1.0 \text{ and } (M_{T_R})_D < 1.0 \\ 63.0 + 20 \text{ Log}(M_{T_R})_D & \text{for } M_{T_R} \leq 1.0 \text{ and } (M_{T_R})_D > 1.0 \\ 63.0 + 20 \text{ Log}[(M_{T_R})_D / M_{T_R}) & \text{for } M_{T_R} > 1.0 \end{cases} \quad \text{(C36)}$$

When inlet guide vanes are present the sound pressure level is increased by 6 dB as indicated by the flow distortion function I(IGV)

$$I(IGV) = \begin{cases} 0 & \text{without inlet guide vanes} \\ 6 & \text{with inlet guide vanes} \end{cases} \quad \text{(C37)}$$

The correction for rotor stator spacing and the spectrum function S(n) are identical to the inlet discrete tone function described by equations C23, C24 and C25.

References

1. Tibbetts, J. G.: A Computer Program for the Prediction of Near-Field Noise of Aircraft in Cruising Flight-User's Guide. NASA Contractor Report 159274, June 1980.

2. Tibbetts, J. G.: Near-Field Noise Prediction for Aircraft in Cruising Flight-Methods Manual. NASA Contractor Report 159105, August 1979.

3. Swift, G. and Mungur P.: A Study of the Prediction of Cruise Noise and Laminar Flow Control Noise Criteria for Subsonic Air Transports. NASA Contractor Report 159104, August 1979.

4. Schubouer, G. B. and Skromstad, H. K.: Laminar-Boundary-Layer Oscillations and Transition on a Flat Plate. NACA TR Report No. 909, 1948.

5. Blankenship, G. L.; Low, J. K. C.; Watkins, J. A. and Merriman, J. E.: Effect of Forward Motion on Engine Noise. NASA CR-134954, October 1977.

6. Blankenship, G. L.: Effect of Forward Motion on Turbomachinery Noise. AIAA 4th Aeroacoustics Conference, Paper No. 77-1346, October 1977.

7. Low, J. K. C.: Effect of Forward Motion on Jet and Core Noise. AIAA 4th Aeroacoustics Conference, Paper No. 77-1330, 1977.

8. Tam, C.: Effects of Forward Flight on Broadband Shock Associated Noise of Supersonic Jets. Engineering Report No. LG84ER0120 Lockheed-Georgia Company, Aug. 1984.

9. Michalke, A. and Michel, U.: Prediction of Jet Noise in Flight from Static Tests. Journal of Sound and Vibrations, 1979.

10. Harper-Bourne, M. and Fisher, M. J.: The Noise from Shock Waves in Supersonic Jets. AGARD CP 131, Paper 11, September 1973.

11. Plumblee, H. E., et al.: Near-Field Noise Analysis of Aircraft Propulsion Systems with Emphasis on Prediction Techniques for Jets. AFFDL-TR-67-43, Aug. 1967.

12. Heidmann, M. F.: Interim Prediction Method for Fan and Compressor Source Noise. NASA TM X-71763, June 1975.

TABLE 1 FULL SCALE MODEL TURBOFAN CONFIGURATION INPUT

Distance from inlet to primary nozzle exit plane	15 feet
Distance between primary and secondary nozzle exit planes	5 feet
Fan	
Number of fan stages	1
No inlet guide vanes	
Fan inlet cross sectional area. $A = (\pi d^2/4)$ $d = 8'$	50.26 ft^2
Relative tip Mach number at design point	1.5
Blade length	3.5
Number of first-stage rotor blades	45
Number of first-stage stator vanes	95
Rotor stator spacing %	26%
Turbine	
Number of rotor blades in last turbine stage	105
Blade tip diameter of last turbine stage	4.0 ft
Primary nozzle exit area	6.0 ft^2
Core	
Total temperature drop across turbine (all stages) at the engine design point	1200°R
Jet	
Primary exhaust nozzle diameter	2.75 ft
No plug in primary nozzle	
Secondary exhaust nozzle diameter	7.0 ft
Ratio of secondary jet area to primary jet area	6.5
Ratio of secondary jet mass flow rate to primary jet mass flow rate	5.0
Broadband Shock	
Primary nozzle equivalent diameter	2.75 ft
Secondary nozzle equivalent diameter	6.44 ft
Secondary nozzle annulus height	2.125 ft

TABLE 2. FLIGHT CONDITION INPUT (ALTITUDE VARIATION)

Altitude, (ft)	20000	25000	30000	35000	40000
Mach No.	.8	.8	.8	.8	.8
Thrust Setting	100%	100%	100%	100%	100%
Density, (lbm/ft^3)	.04080	.03430	.02870	.02380	.01890
Sound Speed, (ft/sec)	1036.93	1016.10	994.85	973.14	968.08
Fan					
Mass Flow Rate, (lbm/sec)	929.56	786.76	655.50	537.95	425.74
RPM's	3302.47	3362.73	3393.65	3391.77	3382.41
ΔT, (°R)	65.61	67.85	69.68	71.12	70.38
Turbine					
PR	3.02	3.07	3.07	3.02	2.98
RPM's	3302.47	3362.73	3393.65	3391.33	3382.41
Core					
Mass Flow Rate, (lbm/sec)	180.67	158.12	134.17	111.26	88.06
Density, (lbm/ft^3)	.46123	.40833	.35227	.29769	.23606
T_{in}, (°R)	1312.16	1298.76	1277.53	1253.49	1249.28
T_{out}, (°R)	2321.67	2333.04	2331.49	2327.17	2326.28
Jet					
V_1, (ft/sec)	1673.75	1755.25	1805.60	1845.80	1854.76
V_2, (ft/sec)	1195.05	1194.26	1186.21	1176.57	1170.44
T_1, (°R)	1251.60	1255.14	1254.30	1253.49	1258.07
T_2, (°R)	570.29	552.46	534.24	515.62	510.27

TABLE 3. FLIGHT CONDITION INPUT (THRUST VARIATION)

Altitude, (ft)	30000	30000	30000	30000	30000
Mach No.	.8	.8	.8	.8	.8
Thrust Setting	100	92	87	78	64
Density, (lbm/ft^3)	.0287	.0287	.0287	.0287	.0287
Sound Speed, (ft/sec)	994.85	994.85	994.85	994.85	994.85
Fan					
Mass Flow Rate, (lbm/sec)	655.50	645.46	632.08	617.53	601.68
RPM's	3393.65	3305.66	3203.48	3097.52	2983.99
ΔT, (°R)	69.68	65.04	60.39	60.39	55.75
Turbine					
PR	3.07	3.06	3.02	2.97	2.89
RPM's	3393.65	3305.66	3203.48	3097.52	2983.99
Core					
Mass Flow Rate, (lbm/sec)	134.17	129.65	123.68	116.48	109.14
Density, (lbm/ft^3)	.35227	.34100	.32689	.31047	.29219
T_{in}, (°R)	1277.53	1254.30	1226.43	1198.55	1170.68
T_{out}, (°R)	2331.49	2251.09	2168.40	2089.55	2011.76
Jet					
V_1, (ft/sec)	1805.60	1725.17	1640.72	1535.44	1429.40
V_2, (ft/sec)	1186.21	1169.29	1152.02	1135.14	1107.87
T_1, (°R)	1254.30	1212.49	1170.68	1128.87	1087.06
T_2, (°R)	534.24	529.59	524.95	524.95	520.30

TABLE 4. FLIGHT CONDITION INPUT (MACH NUMBER VARIATION)

Altitude, (ft)	30000	30000	30000	30000	30000
Mach No.	.5	.6	.7	.8	.9
Thrust Setting	100	100	100	100	100
Density, (lbm/ft^3)	.0287	.0287	.0287	.0287	.0287
Sound Speed, (ft/sec)	994.85	994.85	994.85	994.85	994.85
Fan					
Mass Flow Rate, (lbm/sec)	531.70	566.76	608.16	655.50	708.64
RPM's	3341.76	3368.28	3387.42	3393.65	3378.15
ΔT, (°R)	73.51	75.05	72.35	69.68	71.78
Turbine					
PR	2.93	2.98	3.03	3.07	3.08
RPM's	3341.76	3368.28	3387.42	3393.65	3378.15
Core					
Mass Flow Rate, (lbm/sec)	111.12	117.71	125.52	134.17	143.00
Density, (lbm/ft^3)	.30083	.31585	.33354	.35227	.37145
T_{in}, (°R)	1236.76	1249.42	1261.64	1277.53	1292.11
T_{out}, (°R)	2325.71	2328.76	2328.73	2331.49	2332.12
Jet					
V_1, (ft/sec)	1631.17	1688.88	1747.75	1805.60	1863.72
V_2, (ft/sec)	1012.82	1069.65	1124.96	1186.21	1257.79
T_1, (°R)	1258.38	1258.25	1257.12	1254.30	1253.82
T_2, (°R)	505.95	516.55	524.55	534.24	550.34

TABLE 5. PARAMETER VARIATION WITH ALTITUDE

		Sea Level	20,000	40,000
Temperature	°F	59.00	-12.25	-69.70
Sound Speed	ft/sec	1116.45	1036.93	968.00
Air Density	lbm/ft^3	.0770	.0408	.0189
Density Ratio		1.0	.529	.245
Air Pressure	lb/ft^2	2116.22	973.27	393.13
Pressure Ratio		1.0	.460	.186
Kinematic Viscosity	ft^2/sec	.0001572	.0002623	.0005056
Acoustic Impedance	$lbm/ft^2\text{-}sec^2$	2.672	1.314	.568
Characteristic Acoustic Impedance Ratio		1.0	.495	.214

TABLE 6. PROPULSION NOISE SOURCE OASPL AS A FUNCTION OF ALTITUDE

	FAN				JET MIXING		BROADBAND SHOCK		
ALT.	FORWARD	AFT	TURB	CORE	PRI	SEC	PRI	SEC	TOTAL
OBSERVER LOCATION #1; ϕ = 30°									
20,000	143.2	103.1	114.8	104.8	91.8	104.3	133.1	147.4	148.9
25,000	141.3	101.5	114.1	102.5	93.8	104.9	137.4	147.9	149.0
30,000	139.7	99.8	113.1	99.8	94.7	104.9	138.9	147.8	148.9
35,000	137.5	98.1	112.0	96.8	95.2	104.8	139.5	147.6	148.6
40,000	135.4	95.9	110.8	92.7	94.6	103.8	138.7	146.6	147.5
OBSERVER LOCATION #2; ϕ = 60°									
20,000	135.6	115.1	121.6	111.6	96.8	118.0	138.9	152.3	152.6
25,000	134.6	113.6	120.8	109.4	98.7	118.1	143.2	152.8	153.3
30,000	134.3	111.9	119.9	106.7	99.6	117.6	144.7	152.7	153.4
35,000	132.2	110.1	118.8	103.7	100.1	117.5	145.3	152.6	153.3
40,000	130.1	108.0	117.6	99.6	99.4	116.5	144.5	151.5	152.3
OBSERVER LOCATION #3; ϕ = 90°									
20,000	118.1	121.7	122.7	113.1	101.1	128.9	137.8	145.2	146.1
25,000	117.4	120.2	122.0	110.8	102.9	129.3	142.1	145.7	147.4
30,000	117.4	118.5	121.0	108.1	103.7	129.2	143.6	145.6	147.8
35,000	115.4	116.7	119.9	105.1	104.2	128.9	144.2	145.4	148.0
40,000	113.2	114.6	118.7	101.1	103.5	127.9	143.4	144.4	147.0
OBSERVER LOCATION #4; ϕ = 120°									
20,000	111.5	124.3	116.9	109.5	110.8	128.2	127.4	135.3	137.0
25,000	110.9	122.8	116.1	107.2	112.5	128.7	131.6	135.8	137.9
30,000	111.1	121.1	115.1	104.5	113.2	128.6	133.1	135.7	138.2
35,000	109.0	119.3	114.0	101.5	113.6	128.4	133.7	135.5	138.2
40,000	106.9	117.1	112.8	97.4	112.9	127.4	132.8	134.5	137.3

TABLE 7. PROPULSION NOISE SOURCE OASPL AS A FUNCTION OF THRUST SETTING

	FAN				JET MIXING		BROADBAND SHOCK		
% THRUST	FORWARD	AFT	TURB	CORE	PRI	SEC	PRI	SEC	TOTAL
				OBSERVER LOCATION #1; ϕ = 30°					
100	139.7	99.8	113.1	99.8	94.7	104.9	138.9	147.8	148.9
92	139.1	99.4	113.3	98.9	92.9	104.0	136.5	147.0	148.0
83	138.9	98.9	113.6	97.8	90.8	103.0	133.1	146.1	147.0
74	138.0	97.2	113.7	96.6	87.6	101.6	124.5	144.7	145.6
65	138.0	96.7	113.6	95.3	84.1	99.6	0.	142.6	143.9
				OBSERVER LOCATION #2; ϕ = 60°					
100	134.3	111.9	119.9	106.7	99.6	117.9	144.7	152.7	153.4
92	132.8	111.4	120.1	105.8	97.9	117.4	142.3	151.9	152.4
83	131.5	110.9	120.4	104.7	95.9	116.7	138.9	151.0	151.3
74	131.1	109.3	120.2	103.5	92.8	115.9	130.3	149.7	149.8
65	131.0	108.8	120.4	102.2	89.4	114.6	0.	147.5	147.6
				OBSERVER LOCATION #3; ϕ = 90°					
100	117.4	118.5	121.0	108.1	103.7	129.2	143.6	145.6	147.8
92	115.6	118.0	121.2	107.2	102.1	128.3	141.3	144.8	146.5
83	114.0	117.5	121.5	106.1	100.2	127.2	137.9	143.9	145.0
74	113.9	116.1	121.6	104.9	97.3	126.0	129.3	142.6	142.9
65	113.7	115.6	121.6	103.6	94.1	124.2	0.	140.4	140.6
				OBSERVER LOCATION #4; ϕ = 120°					
100	111.1	121.1	115.1	104.5	113.2	128.6	133.1	135.7	138.2
92	109.2	120.6	115.3	103.6	112.0	127.5	130.8	134.9	137.0
83	107.4	120.1	115.7	102.5	110.3	126.2	127.4	134.0	135.6
74	107.4	118.8	115.7	101.3	107.6	124.8	118.9	132.7	133.7
65	107.2	118.3	115.7	100.0	104.2	122.8	0.	130.6	131.6

TABLE 8. PROPULSION NOISE SOURCE OASPL AS A FUNCTION OF MACH NUMBER

	FAN				JET MIXING		BROADBAND SHOCK		
MACH NO.	FORWARD	AFT	TURB	CORE	PRI	SEC	PRI	SEC	TOTAL
				OBSERVER LOCATION #1; ϕ = 30°					
0.5	131.2	95.4	105.0	90.4	97.0	112.2	117.6	110.1	131.5
0.6	133.6	96.4	106.7	92.7	96.6	110.2	125.8	131.2	136.0
0.7	136.3	97.5	109.5	95.7	96.0	107.7	132.3	140.0	142.0
0.8	139.7	99.8	113.1	99.8	94.7	104.9	138.9	147.8	148.9
0.9	146.7	105.4	119.2	106.4	92.0	101.6	147.4	157.3	158.1
				OBSERVER LOCATION #2; ϕ = 60°					
0.5	120.4	110.3	111.2	96.9	102.6	124.9	121.9	113.4	127.9
0.6	123.9	110.3	112.9	99.1	101.8	123.5	130.3	134.7	136.6
0.7	129.1	110.4	115.9	102.2	100.9	121.3	137.3	143.9	144.9
0.8	134.3	111.9	119.9	106.7	99.6	117.8	144.7	152.7	153.4
0.9	140.9	117.1	126.9	114.1	96.9	112.7	154.5	164.5	164.9
				OBSERVER LOCATION #3; ϕ = 90°					
0.5	112.7	119.6	113.3	100.0	109.0	130.1	121.1	110.2	131.3
0.6	114.5	119.3	114.6	101.5	107.2	129.8	129.4	130.6	135.0
0.7	116.4	118.7	117.2	104.0	105.5	129.5	136.2	138.6	141.0
0.8	117.4	118.5	121.0	108.1	103.7	129.2	143.6	145.6	147.8
0.9	119.4	120.3	128.3	115.7	101.0	128.9	154.2	153.6	156.9
				OBSERVER LOCATION #4; ϕ = 120°					
0.5	108.2	121.7	112.4	101.7	118.0	129.1	115.6	104.6	130.4
0.6	109.5	121.7	112.7	102.3	117.3	128.9	122.8	124.2	131.7
0.7	110.8	121.3	113.8	103.2	116.0	128.7	128.1	130.8	134.5
0.8	111.1	121.1	115.1	104.5	113.2	128.6	133.1	135.7	138.2
0.9	112.1	121.8	117.3	106.6	108.7	128.9	138.9	140.1	142.5

TABLE 9. RELATIVE JET MACH NUMBER VARIATION WITH FLIGHT MACH NUMBER

M_f	V_a	V_j	M_j	$M = M_j(1-V_a/V_j)^{3/4}$
.5	497.43	1631.17	1.05	.79
.6	596.91	1688.88	1.09	.79
.7	693.40	1747.75	1.14	.78
.8	795.88	1805.60	1.19	.77
.9	895.37	1863.72	1.24	.76

TABLE 10. SOURCE RANKING ON OASPL

Noise Source	Observer Angle in degrees			
	30	60	90	120
Broadband Shock (Primary)	*	*	*	*
Broadband Shock (Secondary)	*	*	*	*
Jet Mixing (Secondary)		*	*	*
Fan (Forward)	*	*		
Fan (Aft)		*	*	*

TABLE 11. BROADBAND SHOCK NOISE OASPL AS A FUNCTION OF JET MACH NUMBER; $M_a = 0.$

PRIMARY JET		SECONDARY JET		OASPL BROADBAND SHOCK		
V_j (ft/sec)	T_j(°R)	V_j(ft/sec)	T_j(°R)	M_j	PRIMARY	SECONDARY
1488.29	1150	1016.81	525	.99	0.	0.
1501.21	1150	1025.37	525	1.0	65.0	67.0
1533.25	1150	1046.60	525	1.025	116.2	123.4
1564.95	1150	1067.56	525	1.05	122.4	129.5
1627.30	1150	1108.67	525	1.10	128.6	135.8
1688.26	1150	1148.71	525	1.15	132.3	139.4
1747.81	1150	1187.67	525	1.20	134.9	142.0
1805.95	1150	1225.55	525	1.25	137.0	144.1

TABLE 12. BROADBAND SHOCK NOISE OASPL AS A FUNCTION OF JET MACH NUMBER; $M_a = 0.8$

PRIMARY JET		SECONDARY JET		BROADBAND SHOCK		
V_j (ft/sec)	T_j(°R)	V_j(ft/sec)	T_j(°R)	M_j	PRIMARY	SECONDARY
1488.29	1150	1016.81	525	.99	0.	0.
1501.21	1150	1025.37	525	1.0	84.4	79.9
1533.25	1150	1046.60	525	1.025	130.4	132.2
1564.95	1150	1067.56	525	1.05	136.5	138.4
1627.30	1150	1108.67	525	1.10	142.8	144.7
1688.26	1150	1148.71	525	1.15	146.5	148.5
1747.81	1150	1187.67	525	1.20	149.2	151.2
1805.95	1150	1225.55	525	1.25	151.3	153.3

TABLE A1.

MASTER SPECTRA FOR BROADBAND SHOCK NOISE

σ_i	10 Log (H_i)	C_i
0.2	116.0	0.70
0.3	121.6	0.71
0.4	125.5	0.71
0.7	132.5	0.72
1.0	137.7	0.73
1.5	142.7	0.74
2.0	145.7	0.74
3.0	148.5	0.71
3.5	149.1	0.69
4.0	149.2	0.67
4.5	149.1	0.64
5.0	148.8	0.62
6.0	147.9	0.58
7.0	146.7	0.54
8.0	145.7	0.50
10.0	143.7	0.45
20.0	137.4	0.28
40.0	130.5	0.12
68.0	125.4	0.02
70.0	125.2	0.02

TABLE B1

COEFFICIENTS A(I,J) FOR JET NOISE PARAMETERS

	Frequency Band I			
	1 OVERALL	2 OVERALL	3 OVERALL	4 OVERALL
1	0.8239	0.4176	0.32555	0.74038
2	-1.24	-1.7269	0.2482	-3.4538
3	-2.3019	-1.3226	-4.0206	-4.7181
4	1.4745	1.3507	2.6807	3.2662
5	45.759	18.932	202.88	331.55
6	-2.1086	-3.2199	3.8424	0.53294
7	3.3692	1.3276	10.520	9.5983
8	-2.3864	-0.1765	-8.0248	-6.829
9	12.808	8.4045	10.491	10.429
10	-1.8167	-1.5494	-0.019983	0.36732
11	-1.7894	-0.16571	0.73551	0.89132
12	1.1641	0.22007	-0.76495	-0.87600
13	4.512	5.2846	4.5428	2.6963
14	-0.028729	1.3015	0.20763	1.8687
15	0.789	0.85116	0.27691	3.0174
16	-0.51772	-0.60053	0.036298	-2.1329
17	2.293×10^{14}	1.993×10^{13}	6.086×10^{13}	4.794×10^{13}

TABLE B2

IDENTIFICATION OF FREQUENCY BANDS FOR JET NOISE ESTIMATION

		Hemholtz Number $H_N = fD/c_a$	
Index I	Band	Band Center	Range
1	Overall	1.25	0.078 to 20
2	Octave	0.221	0.156 to 0.312
3	Octave	0.442	0.312 to 0.625
4	Octave	0.884	0.625 to 1.25

TABLE B3.

REDUCED SPECTRA SHAPES FOR NEAR-FIELD JET NOISE

$Y/D \leq 30$				
REDUCED SOUND PRESSURE LEVEL, $L_{A(N)}$ OR $L_{B(N)}$ (dB)				
Strouhal No.	x/D_j			
$S_{A(N)}$ or $S_{B(N)}$	0 → 5*	10	20	30
0.04	23.8	19.9	16.5	13.6
0.05	21.9	18.1	14.9	11.4
0.06	20.5	16.8	13.3	9.9
0.07	19.2	15.6	12.3	8.6
0.08	18.2	14.6	11.4	7.6
0.09	17.3	13.8	10.6	6.8
0.10	16.6	13.0	9.9	6.2
0.12	15.3	11.9	8.9	5.2
0.16	13.4	10.0	7.3	4.1
0.20	11.9	8.6	6.2	3.6
0.25	10.4	7.4	5.3	3.6
0.30	9.2	6.5	4.8	3.8
0.40	7.5	5.3	4.1	4.7
0.50	6.2	4.3	3.8	5.8
0.60	5.2	3.8	3.8	6.8
0.70	4.5	3.2	4.0	7.6
0.80	3.8	3.0	4.2	8.5
0.90	3.4	2.8	4.6	9.2
1.0	3.0	2.6	5.0	10.0
1.2	2.6	2.7	5.6	11.3
1.6	2.2	3.2	6.9	13.6
2.0	2.2	3.8	8.0	15.5
2.5	2.6	4.7	9.3	17.4
3.0	2.9	5.4	10.4	19.2
4.0	3.6	6.8	12.4	21.9
5.0	4.2	7.9	14.0	24.1
6.0	4.9	9.0	15.5	26.0
7.0	5.5	10.0	16.6	27.5
8.0	6.0	10.9	17.7	28.9
9.0	6.6	11.7	18.7	30.1
10.0	7.1	12.4	19.5	31.4

*These values are assumed to apply to the forward quadrant up to $X/D \geq -30$.

TABLE B4.

CORRECTION FACTOR (M_c) FOR THE PRIMARY JET NOISE OF COAXIAL JETS

$\log_{10}[\frac{f(I)D_j}{V_j}]$	M_c AREA RATIO (AR)				
	1	3	6	10	15
-1.15	2.00	0.85	0.00	0.00	0.95
-1.00	1.22	0.80	0.66	0.74	1.60
-0.8	0.46	1.02	1.45	1.66	2.63
-0.6	0.74	1.34	2.16	2.46	3.60
-0.2	1.41	2.07	3.47	3.74	4.77
0.0	1.78	2.49	4.07	4.23	4.99
0.2	2.16	2.93	4.62	4.62	5.02
0.4	2.55	3.38	4.97	4.91	5.03
0.6	2.95	3.85	5.04	5.04	5.04
0.8	3.36	4.31	5.06	5.06	5.06
1.0	3.80	4.72	5.08	5.08	5.08
1.2	4.24	5.04	5.10	5.10	5.10
1.4	4.70	5.10	5.10	5.10	5.10
1.6	5.00	5.10	5.10	5.10	5.10
1.8	5.10	5.10	5.10	5.10	5.10
2.0	5.10	5.10	5.10	5.10	5.10

f(I) = Primary jet frequencies, I = 1, 2, 3, 4

TABLE C1. FAN NOISE DIRECTIVITY

ΔdB CORRECTIONS					
Angle From Inlet (Deg) ϕ'	Broadband		Discrete Tones		
	Inlet	Discharge	Inlet	Discharge	CTN
0	-2.2	-41.7	-2.9	-38.8	-9.5
10	-1.0	-37.4	-1.5	-34.8	-8.5
20	0	-33.1	0	-30.8	-7.0
30	0	-28.8	0	-26.8	-5.0
40	0	-24.3	0	-22.8	-2.0
50	-2.0	-20.1	-1.2	-18.9	0
60	-4.5	-15.8	-3.5	-15.0	0
70	-7.5	-11.5	-6.8	-11.0	-3.5
80	-11.0	-8.0	-10.5	-8.0	-7.5
90	-15.0	-5.0	-14.5	-5.0	-9.0
100	-19.5	-2.7	-19.0	-3.0	-9.5
110	-25.0	-1.2	-23.3	-1.0	-10.0
120	-30.6	-0.3	-27.8	0	-10.5
130	-36.3	0	-32.4	0	-11.0
140	-42.1	-2.0	-36.9	-2.0	-11.5
150	-47.6	-6.0	-41.5	-5.5	-12.0
160	-53.3	-10.0	-46.0	-9.0	-12.5
170	-58.8	-15.0	-50.4	-13.0	-13.0
180	-64.6	-20.0	-55.0	-18.0	-13.5

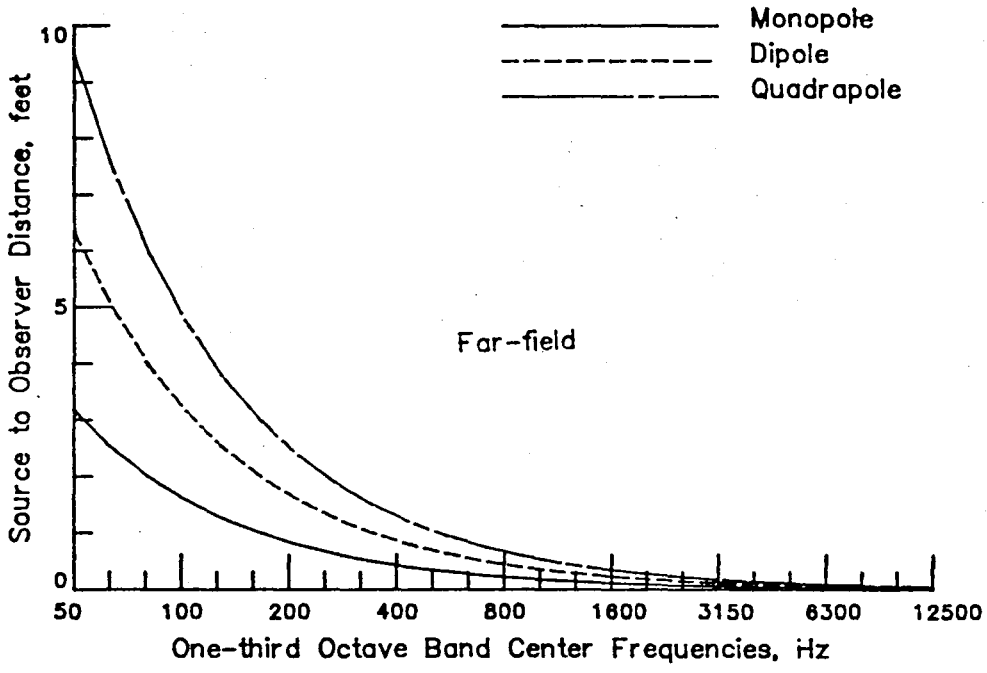

Figure 1. Division of acoustic near and far-field.
Altitude = 30,000 feet; Sound speed = 994.85 ft/sec.

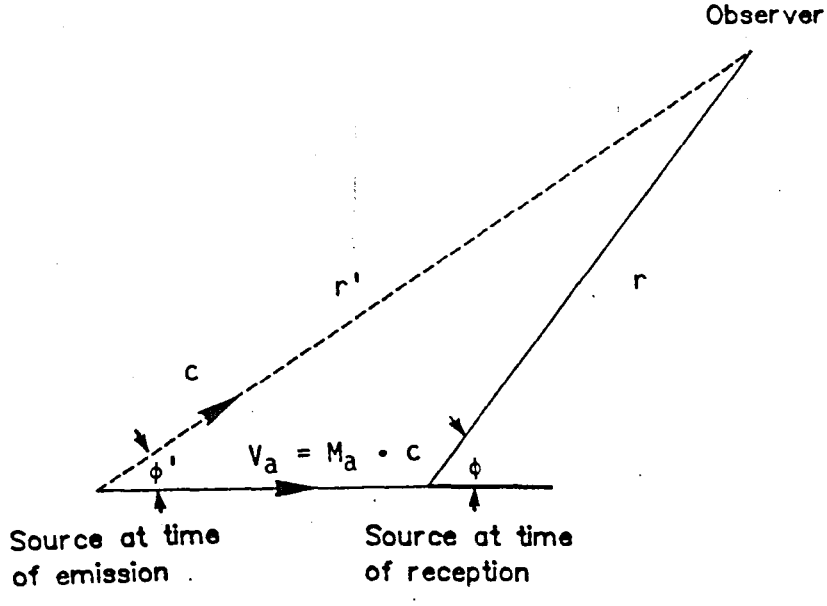

Figure 2. Cruise coordinate transformation.

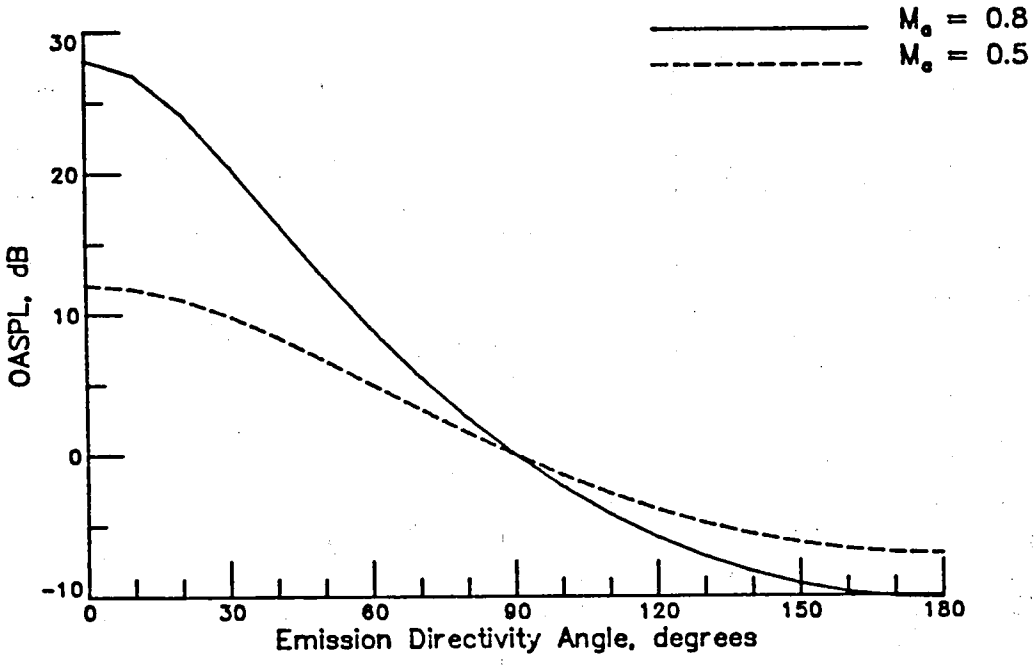

Figure 3. Convective amplification.

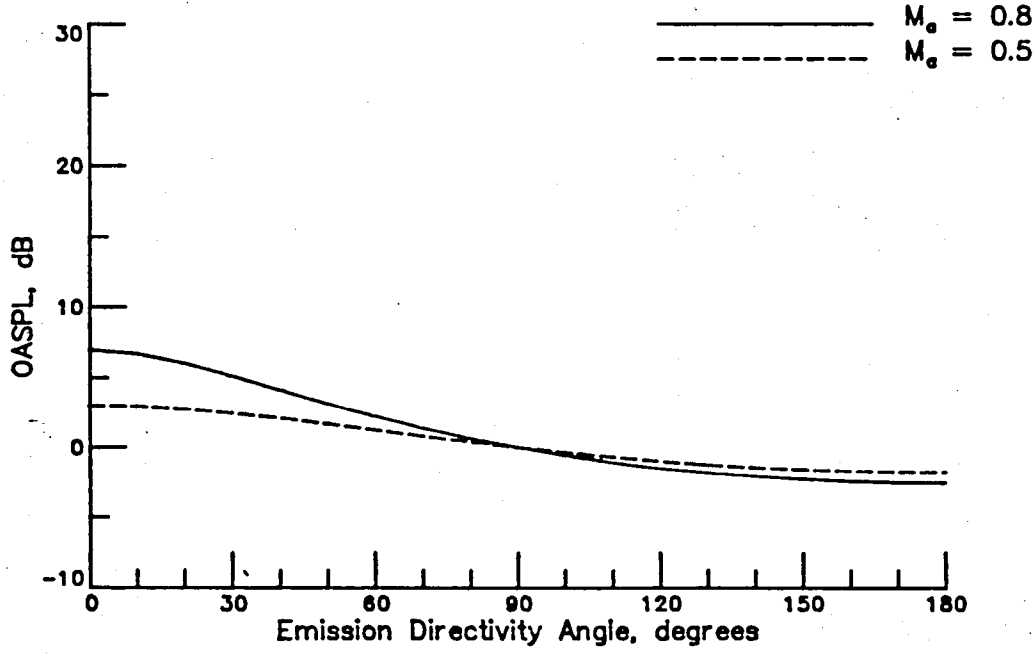

Figure 4. Dynamic amplification.

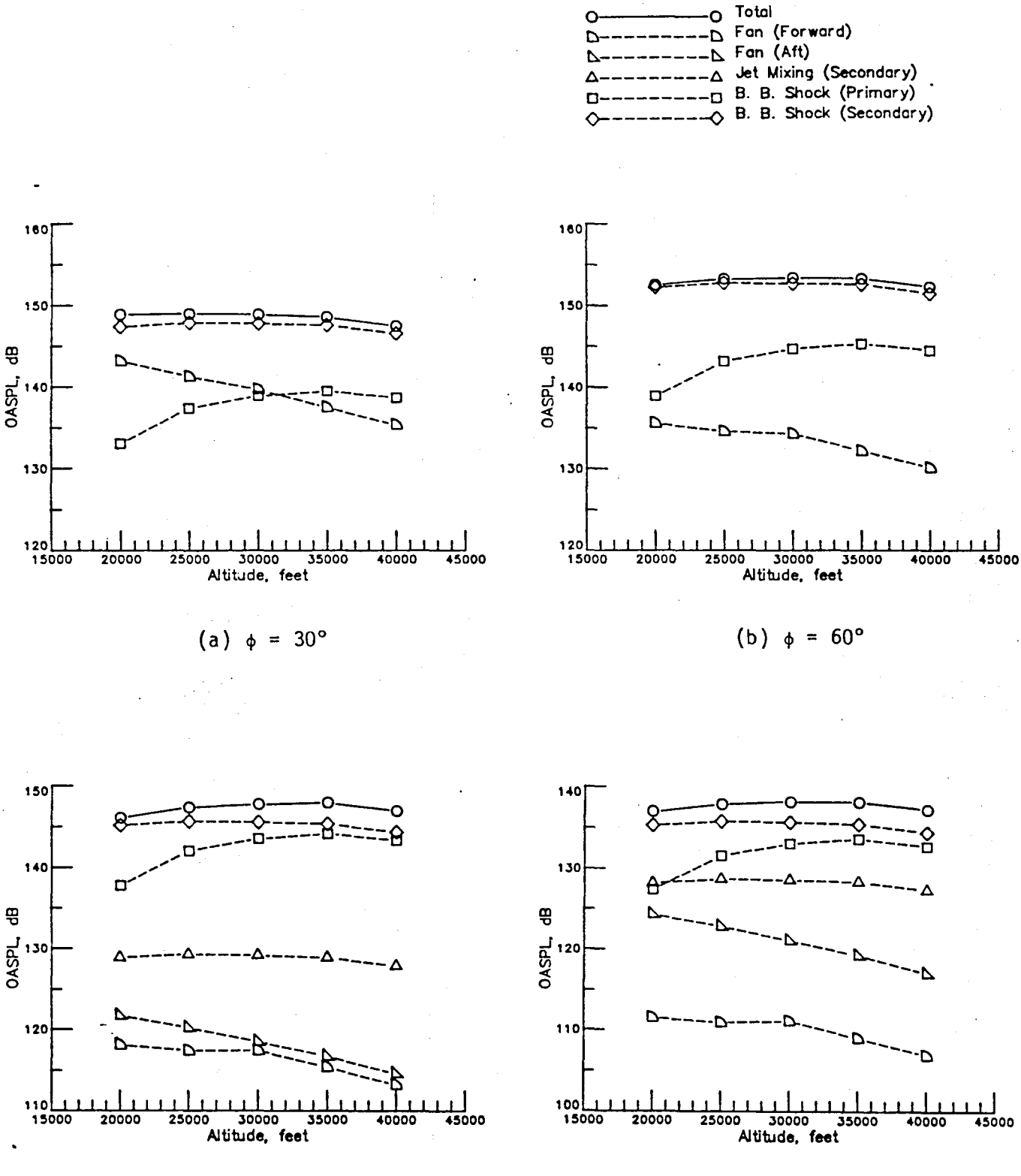

Figure 5. Propulsion noise source OASPL as a function of altitude: M_a = 0.8; Thrust = 100%.

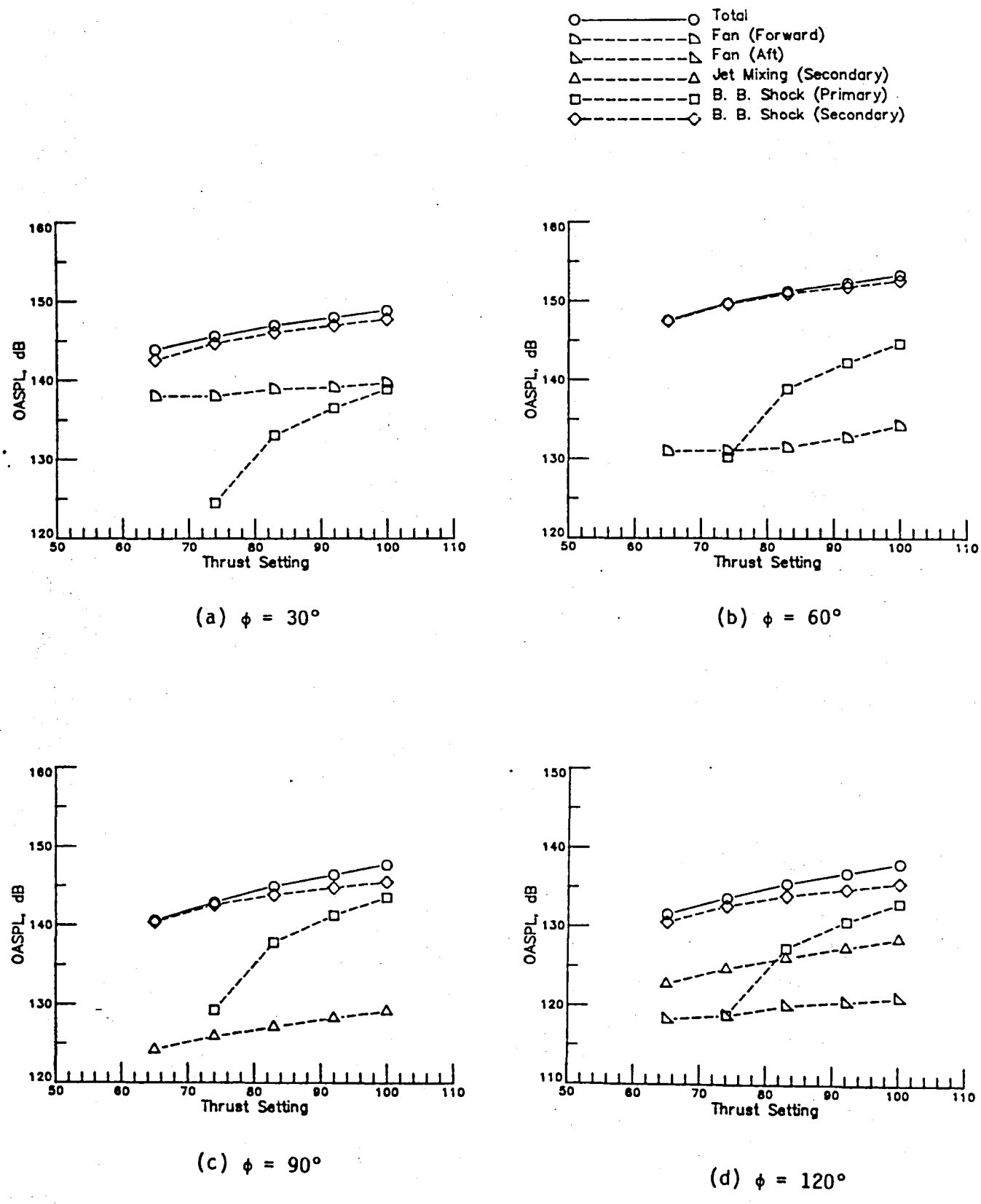

Figure 6. Propulsion noise source OASPL as a function of thrust setting: M_a = 0.8; Altitude = 30,000 feet.

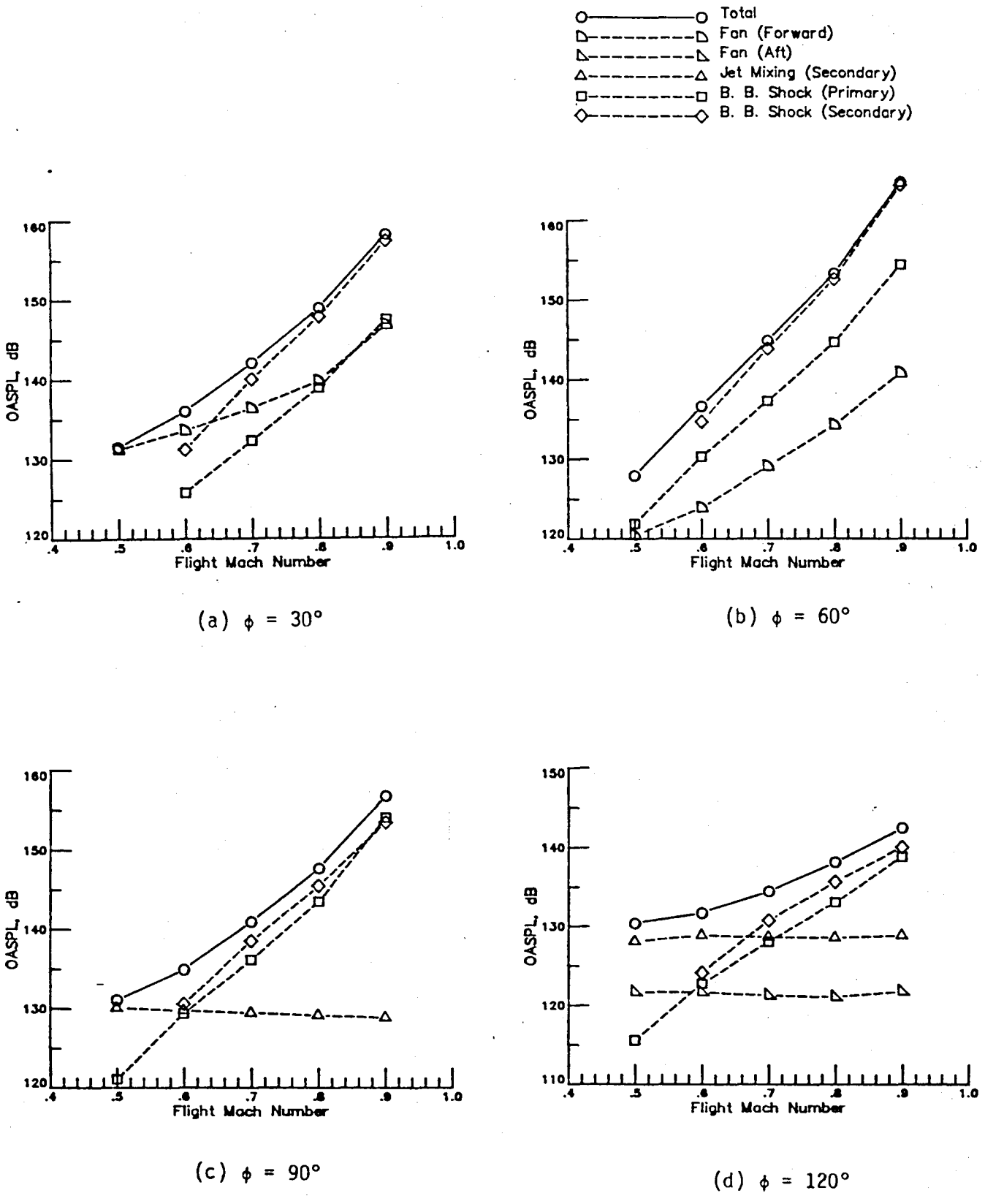

Figure 7. Propulsion noise source OASPL as a function of flight Mach number: Thrust = 100%; Altitude = 30,000 feet.

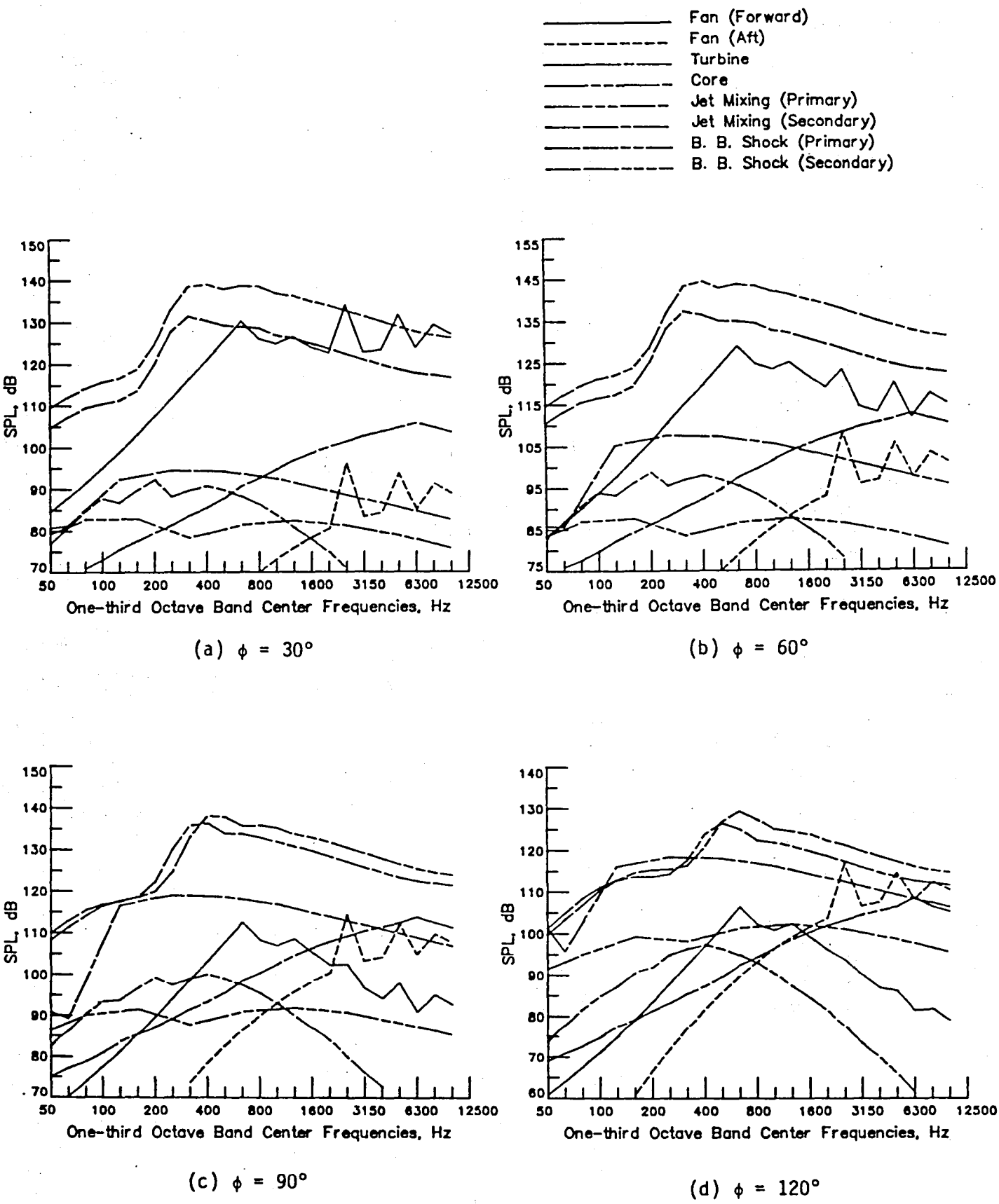

Figure 8. Propulsion noise source one-third octave band spectra: Altitude = 30,000 feet; Thrust = 100%; M_a = 0.8.

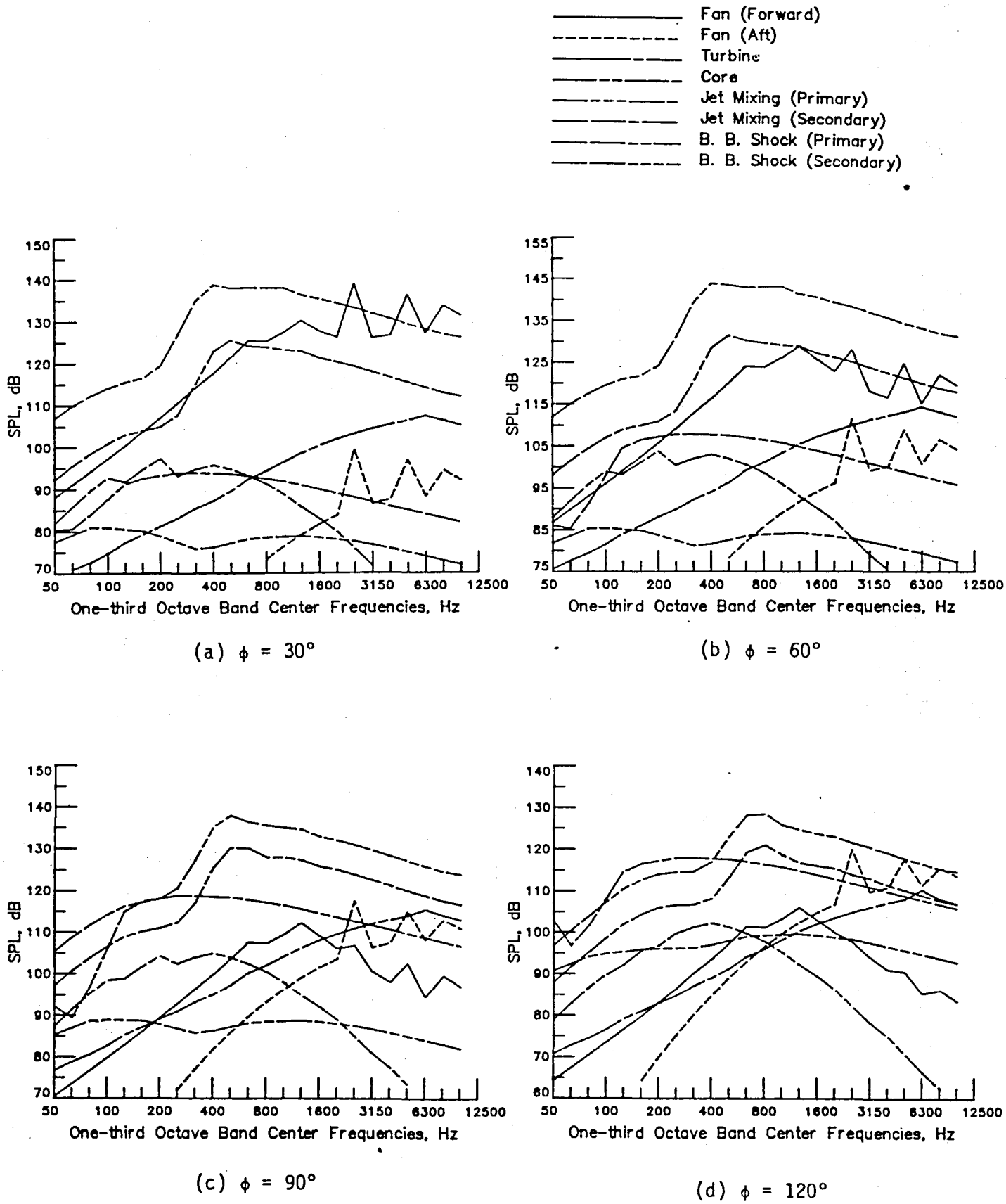

Figure 9. Propulsion noise source one-third octave band spectra: Altitude = 20,000 feet; Thrust = 100%; M_a = 0.8.

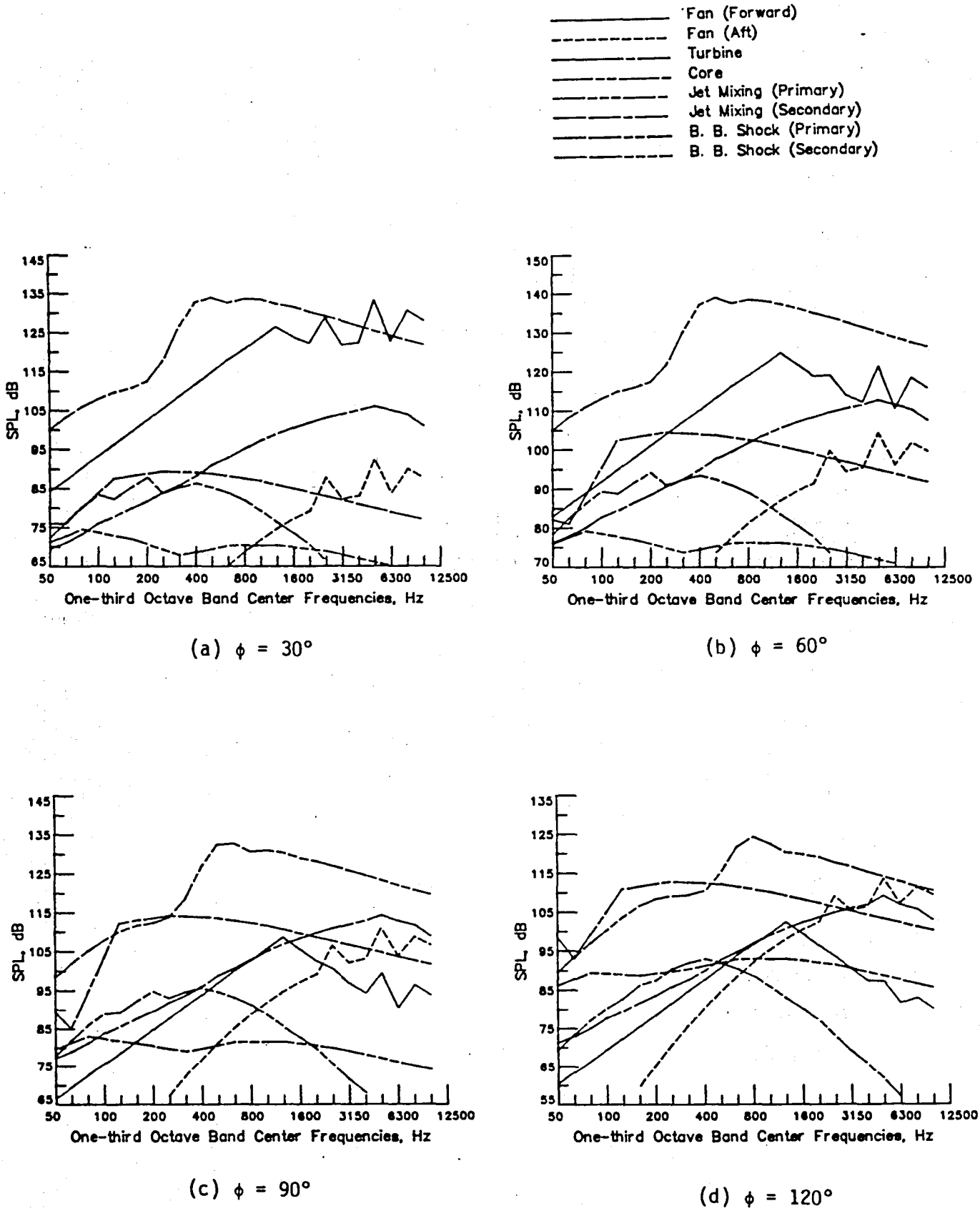

Figure 10. Propulsion noise source one-third octave band spectra: Altitude = 30,000 feet; Thrust = 64%; M_a = 0.8.

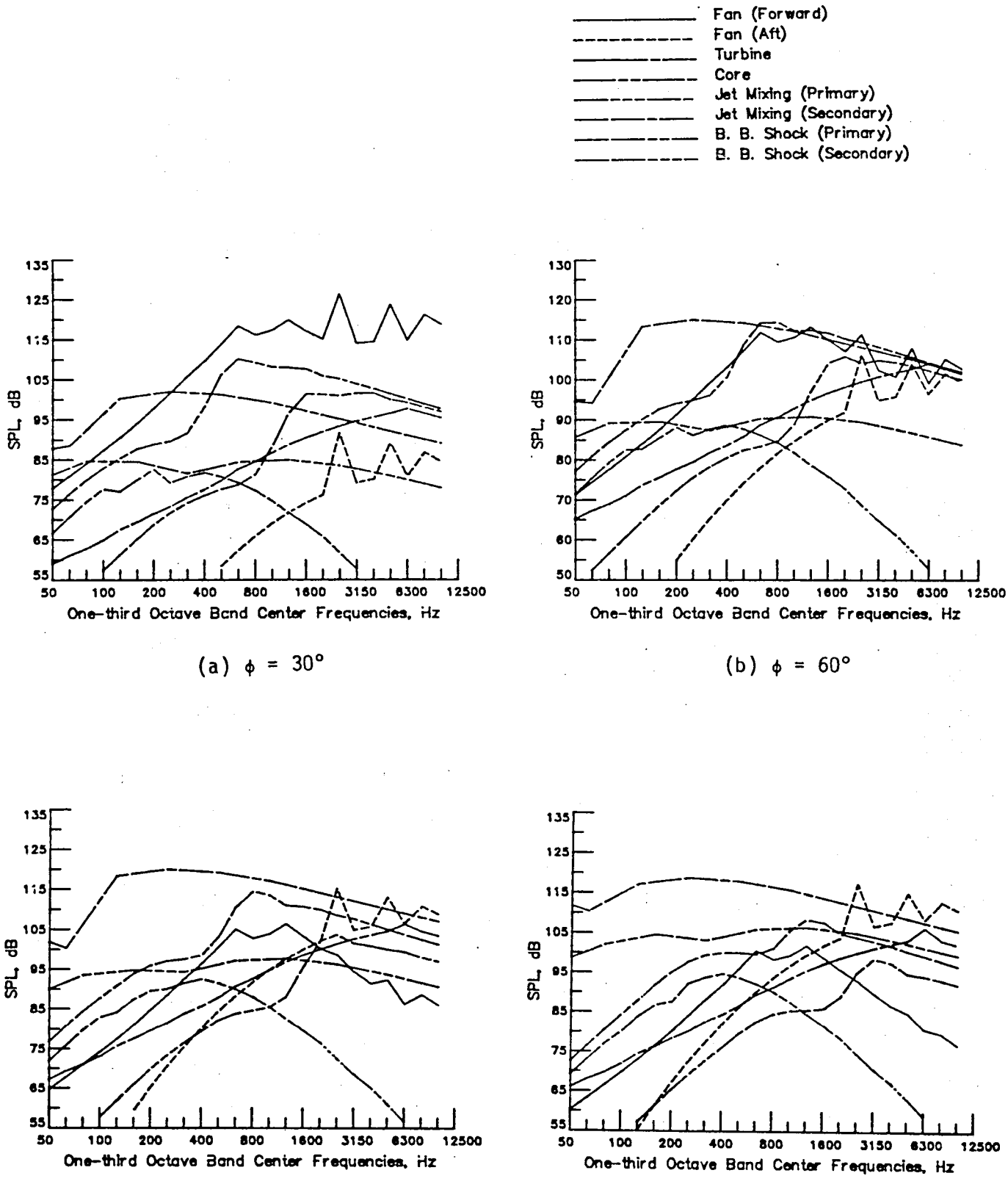

Figure 11. Propulsion noise source one-third octave band spectra: Altitude = 30,000 feet; Thrust = 100%; M_a = 0.5.

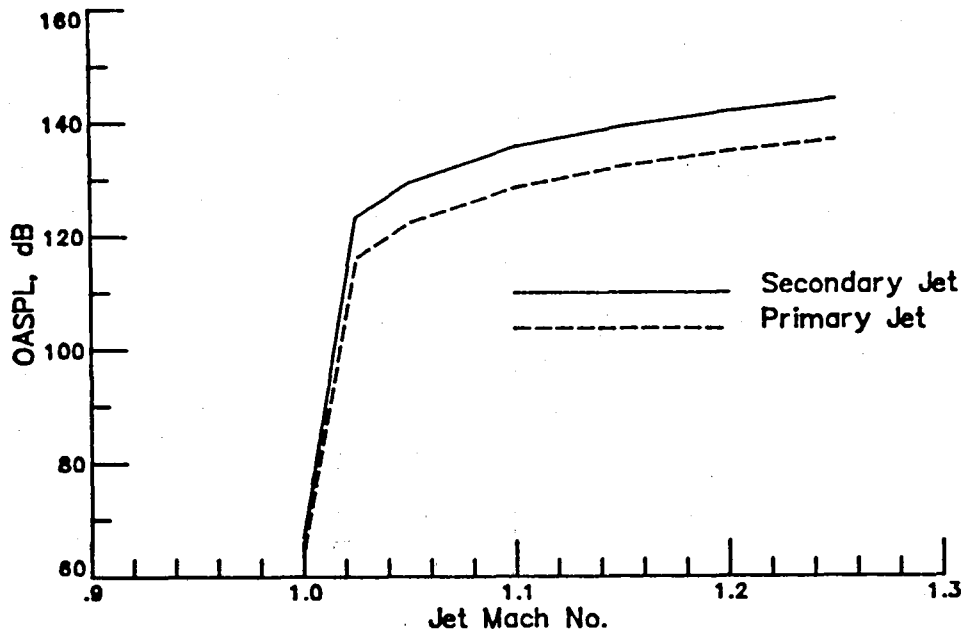

Figure 12. Broadband shock noise OASPL as a function of jet Mach number: $M_a = 0$; $\phi = 90°$; $\phi' = 90°$.

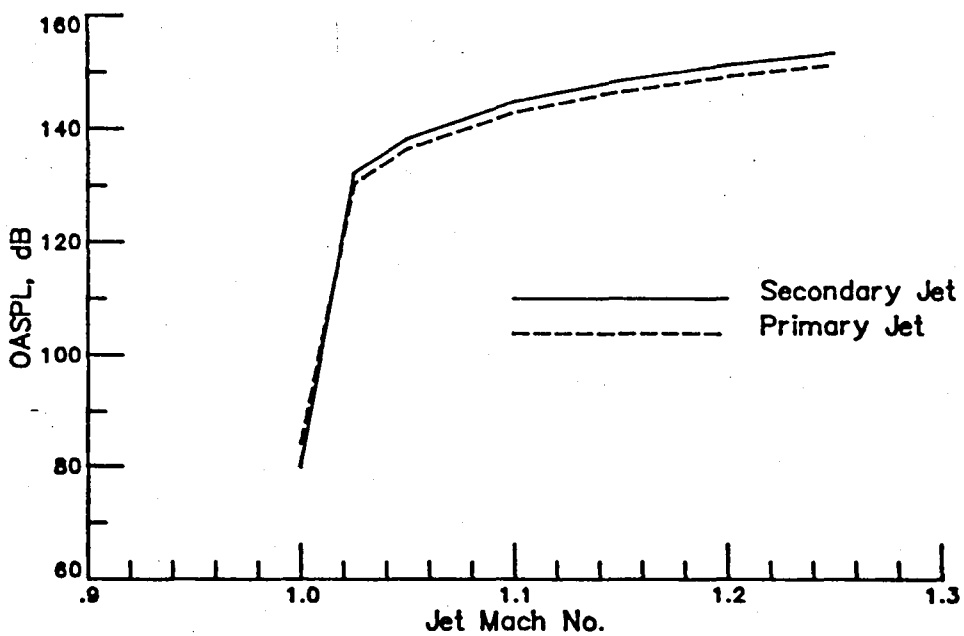

Figure 13. Broadband shock noise OASPL as a function of jet Mach number: $M_a = 0.8$; $\phi = 90°$; $\phi' = 36.9°$.

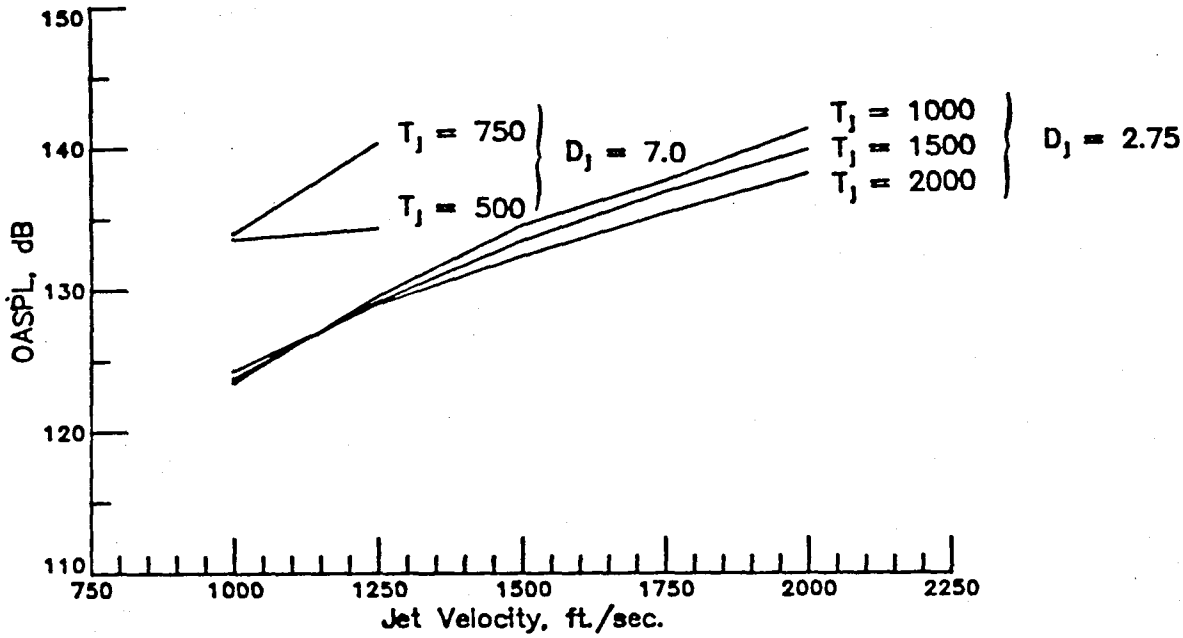

Figure 14. Jet mixing noise OASPL as a function of jet velocity: $M_a = 0$; $\phi = 120°$; $\phi' = 120°$.

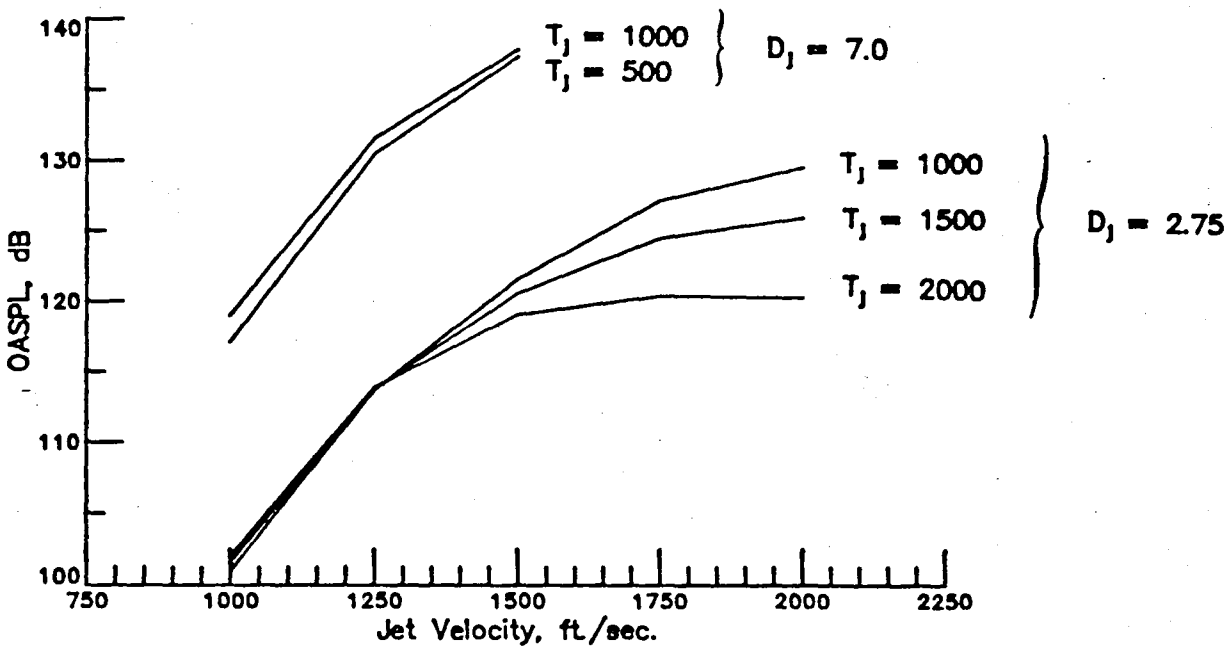

Figure 15. Jet mixing noise OASPL as a function of jet velocity: $M_a = 0.8$; $\phi = 120°$; $\phi' = 76.1°$.

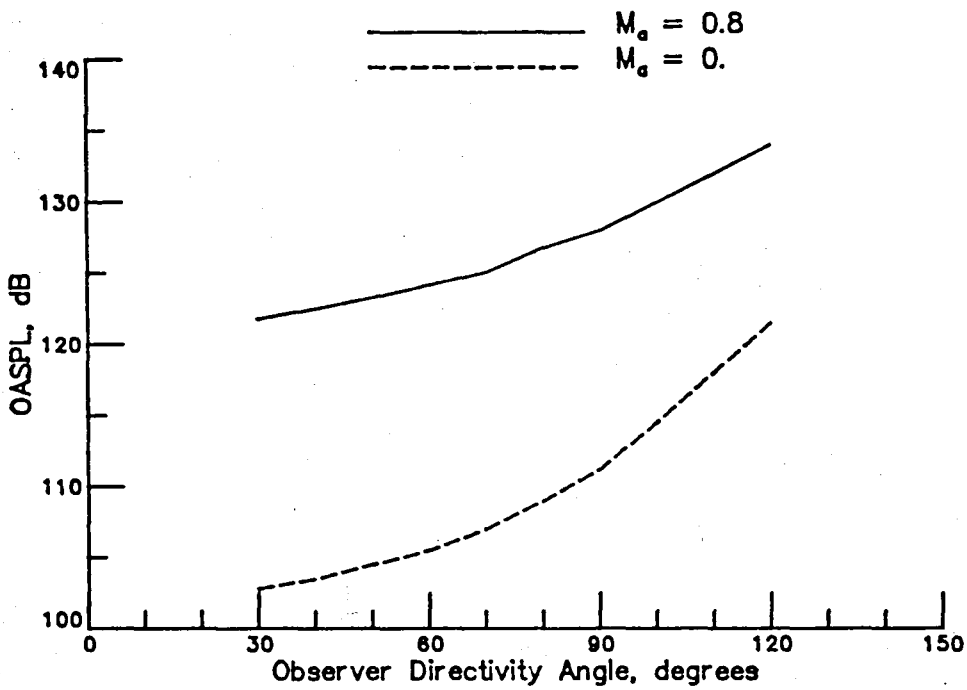

Figure 16. Jet mixing noise OASPL as a function of observer angle.

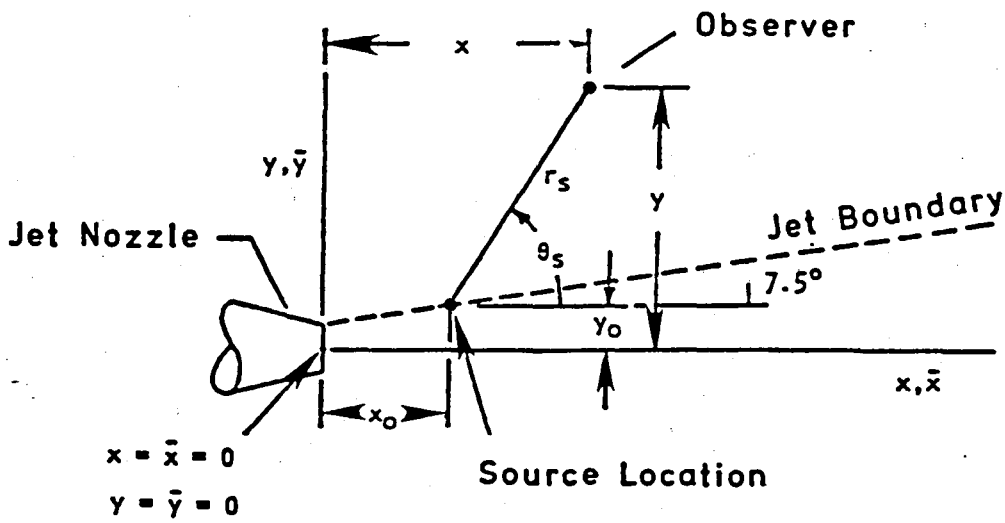

Figure 17. Source and observer geometry for jet mixing noise.

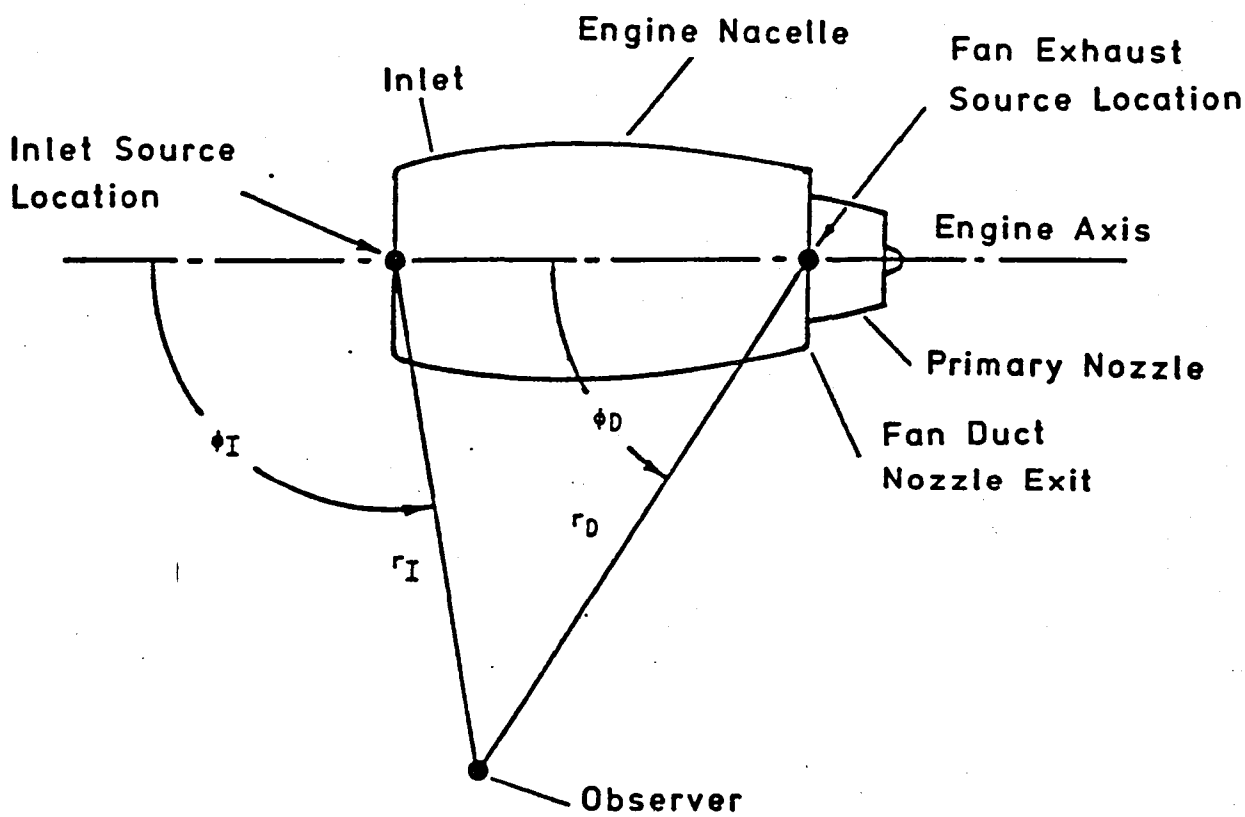

Figure 18. Engine noise source location relative to observer.

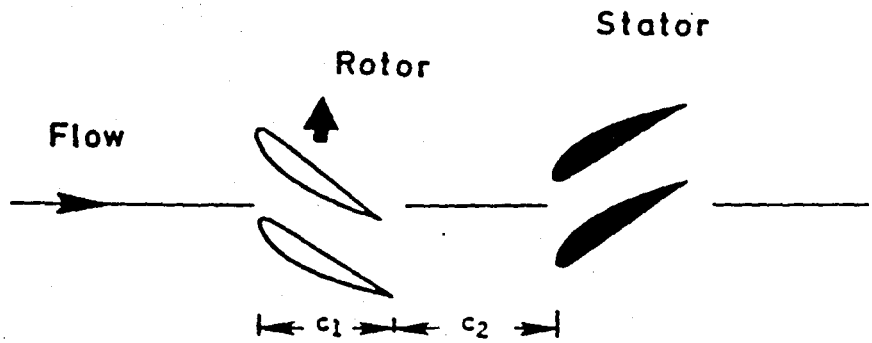

$$RSS = (c_2/c_1) \times 100$$

(a) Fan first stage without inlet guide vanes.

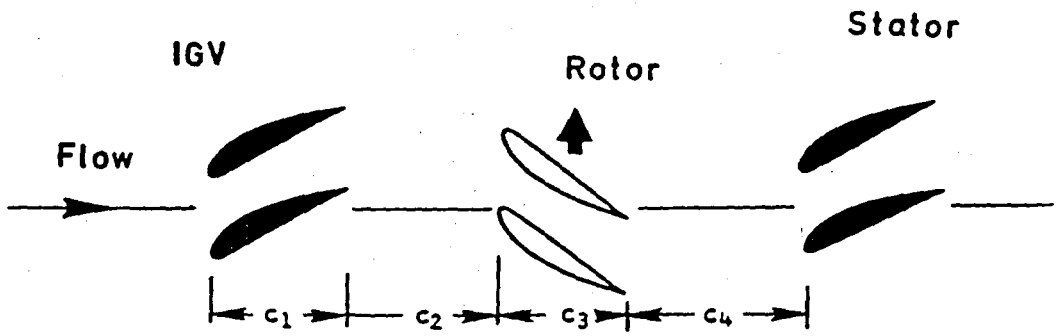

RSS = Minimum of $(c_2/c_1) \times 100$ or $(c_4/c_3) \times 100$

(b) Fan first stage with inlet guide vanes or for second stage.

Figure 19. Fan rotor-stator spacing geometry.

Standard Bibliographic Page

1. Report No.	2. Government Accession No.	3. Recipient's Catalog No.
NASA CR-178146		

4. Title and Subtitle	5. Report Date
Noise Predictions of a High Bypass Turbofan Engine Using the Lockheed Near-Field Noise Prediction Program	July 1986
	6. Performing Organization Code
7. Author(s)	8. Performing Organization Report No.
John W. Rawls, Jr.	
9. Performing Organization Name and Address	10. Work Unit No.
PRC Kentron, Inc. Aerospace Technologies Division 3221 North Armistead Avenue Hampton, VA 23666	11. Contract or Grant No. NAS1-18000
12. Sponsoring Agency Name and Address	13. Type of Report and Period Covered
National Aeronautics and Space Administration Washington, DC 20546	Contractor Report
	14. Sponsoring Agency Code 505-60-31-07

15. Supplementary Notes

Langley Technical Monitor: J. A. Schoenster

16. Abstract

This report examines the prediction of engine noise during cruise using the Near-Field Noise Prediction Program developed by Lockheed. Test conditions were established which simulate the operation of a high bypass turbofan engine under a wide range of operating conditions. These test conditions include variations in altitude, flight Mach number and thrust setting. Based on the results of noise prediction made using the Lockheed program, an evaluation of the impact of these test conditions on the OASPL and the one-third octave band spectra is made. An evaluation of the sensitivity of flight condition parameters is also made.

The primary noise source from a high bypass turbofan was determined to be fan broadband shock noise. This noise source can be expected to be present during normal cruising conditions. When present, fan broadband shock noise usually dominates at all frequencies and all directivity angles. Other noise sources of importance are broadband shock noise from the primary jet, fan noise, fan mixing noise and turbine noise.

17. Key Words (Suggested by Authors(s))	18. Distribution Statement
near field noise prediction jet engine noise prediction noise sensitivity to flight conditions	Unclassified - Unlimited Subject Category 71

19. Security Classif.(of this report)	20. Security Classif.(of this page)	21. No. of Pages	22. Price
Unclassified	Unclassified	70	A04

For sale by the National Technical Information Service, Springfield, Virginia 22161

End of Document